

An Analytic Layer-wise Deep Learning Framework with Applications to Robotics

Huu-Thiet Nguyen¹, Chien Chern Cheah¹, and Kar-Ann Toh²

¹School of Electrical and Electronic Engineering, Nanyang Technological University, 50 Nanyang Avenue, Singapore 639798

²School of Electrical and Electronic Engineering, Yonsei University, Seoul, Korea 03722

Abstract

Deep learning has achieved great success in many applications, but it has been less well analyzed from the theoretical perspective. To deploy deep learning algorithms in a predictable and stable manner is particularly important in robotics, as robots are active agents that need to interact safely with the physical world. This paper presents an analytic deep learning framework for fully connected neural networks, which can be applied for both regression problems and classification problems. Examples for regression and classification problems include online robot control and robot vision. We present two layer-wise learning algorithms such that the convergence of the learning systems can be analyzed. Firstly, an inverse layer-wise learning algorithm for multilayer networks with convergence analysis for each layer is presented to understand the problems of layer-wise deep learning. Secondly, a forward progressive learning algorithm where the deep networks are built progressively by using single hidden layer networks is developed to achieve better accuracy. It is shown that the progressive learning method can be used for fine-tuning of weights from convergence point of view. The effectiveness of the proposed framework is illustrated based on classical benchmark recognition tasks using the MNIST and CIFAR-10 datasets and the results show a good balance between performance and explainability. The proposed method is subsequently applied for online learning of robot kinematics and experimental results on kinematic control of UR5e robot with unknown model are presented.

1 Introduction

Artificial neural networks (ANNs), or simply neural networks (NNs), have been widely deployed in data related problems, such as regression analysis, classification, data processing, control and robotics, etc. In robotic applications, the use of ANNs can be traced back to late 1980s [1]. The ANNs have been proved to be universal approximators [2, 3] where their great potential in identification and control of dynamic systems was discussed in [4]. Hence, they have been regarded as a potential approach to deal with nonlinearities, modeling uncertainties and disturbances in robot control systems.

For years, many results in feedback control of robots have been obtained by focusing on regression problems based on *simple shallow networks*. Most studies are based on one hidden layer networks such as the single-hidden layer feedforward networks (SLFNs) and radial basis function networks (RBFNs). There are two notable approaches in learning of these networks in robotics:

the first approach is training only the output weights, which is still popular until recently [5–11]; the second approach focuses on training both input and output weights of the network [12–15].

In the first approach of training only the output weights, by using linear output activation functions, the algorithms for updating the last layer of weights of these networks resemble those adaptive control techniques where the output equation is linear with tunable parameters. Similar to the adaptive control, the convergence and stability of these algorithms can be ensured by using the Lyapunov method. Among those early studies in NN based control, Sanner and Slotine [5] analyzed the approximation capability of Gaussian networks and employed them in control of systems with dynamic uncertainties. The RBFNs were employed in an indirect controller of a subsystem and in an adaptive NN model reference controller of another subsystem in underactuated wheeled inverted pendulums [6]. While robot control problems are usually formulated for trajectory tracking task, a region adaptive NN controller with a unified objective bound was synthesized for robot control in task space [7]. In [8], He et al. proposed an adaptive NN control technique for robots with full-state constraints which guaranteed the asymptotic tracking. Global stability was ensured by using a NN-based controller for dual-arm robots with dynamic uncertainties [9]. Recently, the approach has been adopted for indirect herding [10]. For robots with unknown Jacobian matrix, [11] proposed SLFN-based controllers that guaranteed the stability of the system.

In the second approach of training weights in both layers, besides the output weights, the input weights of the network are also adjusted. In the 1990s, Chen and Khalil [12] provided convergence analysis of a learning algorithm that was based on the backpropagation (BP) and gradient descent (GD) in multilayer NN control of nonlinear systems. In 1996, Lewis et al. [13] proposed a learning algorithm for updating 2 layers of weights (input weights and output weights) in a SLFN with Lyapunov-based convergence analysis. The study paved the way for more research works in applying SLFNs in dynamic systems like robotics. In [14], control of nonholonomic mobile robots was studied and a NN controller was introduced to deal with disturbances and unmodeled dynamics. In [15], an adaptive NN-based controller was also proposed for manipulators with kinematic and dynamic uncertainties. However, all these works focused on theoretical analysis of shallow networks for dynamic systems (of the form $\dot{z} = f(z)$) and the output activation functions for the networks were also assumed to be linear.

Deep networks [16,17] can achieve better performance as compared to the shallow counterparts when it comes to number of tunable parameters and overfitting problems [18,19]. The deep NNs have been shown to be more powerful in function approximation and classification than the single hidden layer networks [20]. The current boom of machine learning (ML) applications in many aspects of our life is greatly attributed to deep learning (DL) algorithms [21,22] in which backpropagation (BP) [23] plays a major role. DL has replaced many conventional learning algorithms which saw disadvantages in processing raw data [24]. Many unprecedented successes in image recognition have been achieved by the convolutional neural networks (CNNs) [24,25]. However, DL has not less analyzed from theoretical perspective and DL models remain difficult to understand despite tremendous successes [26].

Various attempts have been done to understand the properties of deep networks. Layer-wise learning is one of the methods to dissect a large network into smaller pieces. One method of training network layer-by-layer is using matrix pseudoinverse as in [27] and together with functional inverse, as developed in [28]. The method [28] does not require any computation of the gradient information and can be applied to both regression and classification problems. However, its performance still lags behind the state-of-art gradient descent DL algorithms in many applications. Employing the

layer-wise method in [28], an iterative learning algorithm for offline regression problem of robot kinematics was developed [29] but it was again limited to shallow networks with one or two hidden layers. The algorithm [29] was built and analyzed in continuous time and hence could not be generalized for classification problems. In addition, the learning of the input layer was ignored and the weights obtained were time-varying which thus required averaging. Another approach for training deep networks layer-wisely is greedy layer-wise learning which can be found in network pre-training [30, 31] and forward thinking algorithm [32]. In this methodology [30–32], training of the multilayer NN is performed by adding the layers in a forward manner, starting from the first layer based on the training of shallow networks. Each hidden layer is added a time, and each training step involves only a single hidden layer feedforward network. After training the SLFN in each layer, the input weights are kept while the output weights are discarded. A new hidden layer is then added on top of the hidden layer of the last SLFN to create a new SLFN. However, despite the good performance especially in classification problems, there is no convergence analysis on these algorithms [30–32], which is a common problem in the ML literature.

Robots are active agents which interact physically with the real world, and applying DL tools in robot control need careful consideration [33]. When employing a deep network in control of robotic systems, one should guarantee the stability, convergence and robustness because robots need to be operated in a safe and predictable manner. Most DL algorithms used in ML community lack theoretical supports for convergence analysis. Therefore, in spite of many elegant results from ML research, very few can be directly used in the area of robot control for the reason of safety. Recently, there has been an increasing need of building interpretable and understandable deep neural networks [34]. As a result, the field of explainable artificial intelligence (XAI) has begun to attract more attention from academics [35]. An XAI project launched by DARPA has aimed for developing accountable AI with a compromise between performance and explainability [36]. Therefore establishing a reliable theoretical framework for constructing and training deep networks, which ensures the convergence, could open up many XAI applications to robotics.

This paper aims to develop a theoretical framework for multilayer NNs which can be efficiently applied in operations of robotic systems. Our main focus is on the study of learning algorithms and training methodologies for multilayer NNs to make them perform in a reliable and explainable manner, which is desirable for control of active agents like robots. To achieve that, an inverse learning algorithm is first formulated to understand the issues and difficulties of establishing analytic layer-wise deep learning and based on this study, an analytic forward progressive algorithm is finally proposed to overcome the problems. The main contributions of this paper are:

- i, The development of a theoretical framework to ensure the convergence of the layer-wise deep learning algorithms. To the best of our knowledge, there is currently no theoretical result for analysis of deep learning of fully connected neural networks to ensure convergence for safe operation of robot systems.
- ii, The development of a forward progressive layer-wise learning algorithm for deep networks in which the general input-output function $\mathbf{y} = \mathbf{f}(\mathbf{z})$ is also considered. Based on the convergence analysis, it is shown that the proposed algorithm can be used for fine-tuning of weights.
- iii, The development of a systematic learning or training methodology in which deep networks can be built gradually for reliable operations in both online and offline robotic applications.

The proposed framework is applied to two recognition tasks using the MNIST [37] and CIFAR-10 [38] databases and an online kinematic robot control task using the UR5e manipulator. Experimental results are presented to illustrate the performance of the proposed algorithm. It is shown that forward progressive learning can achieve similar accuracy as compared to gradient descent method but the main advantage is that the convergence of proposed algorithm can be established in a systematic way.

2 Problem Statement

Consider a mapping between the input variable $\mathbf{z} \in \mathbb{R}^m$ and the output variable $\mathbf{y} \in \mathbb{R}^p$

$$\mathbf{y} = \mathbf{f}(\mathbf{z}) \quad (1)$$

The function $\mathbf{f} : \mathbb{R}^m \rightarrow \mathbb{R}^p$ is assumed to be unknown, but can be approximated by available input and output (target) data which are referred to as training data. Our objective is to develop a theoretical framework to achieve an approximation (model) of the function \mathbf{f} based on the training data, so that this model can predict well on unknown new data.

Based on the output variable \mathbf{y} , the problem can be divided into two main types:

- When \mathbf{y} is a continuous variable, the problem is known as a regression problem.
- When \mathbf{y} is a categorical variable, the problem is known as a classification problem.

In the area of robotics, both types of problem can be found. For instance, when a robot needs to identify (and label) the objects within its work space, a classification or a recognition task should be done; but how the robot makes movement by rotating its joints to reach the position of the object would be a regression problem.

In order to approximate \mathbf{f} , a multilayer feedforward neural network (MLFN) is used. In this paper, we present two techniques for training the MLFNs. The first one is called *inverse layer-wise learning* which is presented in section 3. The second one is called *forward progressive learning* which is presented in section 4.

An illustration of an n -layer MLFN ($n - 1$ hidden layers) is shown in Fig. 1. In this MLFN, the number of hidden units for the j^{th} hidden layer ($1 \leq j \leq n - 1$) is denoted as h_j ; the activation functions for the j^{th} hidden layer are denoted as ϕ_j : $\phi_j = [\phi_{j,1}, \phi_{j,2}, \dots, \phi_{j,h_j}]^T$; the activation functions for output layer are denoted as ϕ_n : $\phi_n = \sigma = [\sigma_{i,1}, \sigma_{i,2}, \dots, \sigma_{i,p}]^T$ (and hence $h_n \triangleq p$); The n weight matrices are denoted (from input layer to output layer) as $\mathbf{W}_1, \mathbf{W}_2, \dots, \mathbf{W}_n$ where \mathbf{W}_1 is the matrix of input weights and \mathbf{W}_n is the matrix of output weights. The output of the MLFN as shown in Fig. 1 is given as follows

$$\mathbf{y}_{\mathcal{NN}} = \phi_n(\mathbf{W}_n \phi_{n-1}(\mathbf{W}_{n-1} \phi_{n-2}(\dots \mathbf{W}_3 \phi_2(\mathbf{W}_2 \phi_1(\mathbf{W}_1 \mathbf{z})))) \quad (2)$$

Since the weights are the tunable parameters, the output of the MLFN in (2) can be written as

$$\mathbf{y}_{\mathcal{NN}} = \mathbf{y}_{\mathcal{NN}}(\mathbf{W}_j|_{j=1}^n, \mathbf{z}) \quad (3)$$

The denotation shows the dependence of the network output on the weights \mathbf{W}_j ($j = 1, \dots, n$) and the input variable \mathbf{z} . The output after the $(j - 1)^{\text{th}}$ hidden layer (activation values after ϕ_{j-1}) is given as

$$\mathbf{y}_{\mathcal{NN}(j-1)}(\mathbf{W}_l|_{l=1}^{j-1}, \mathbf{z}) = \phi_{j-1}(\mathbf{W}_{j-1} \phi_{j-2}(\dots \mathbf{W}_3 \phi_2(\mathbf{W}_2 \phi_1(\mathbf{W}_1 \mathbf{z})))) \quad (4)$$

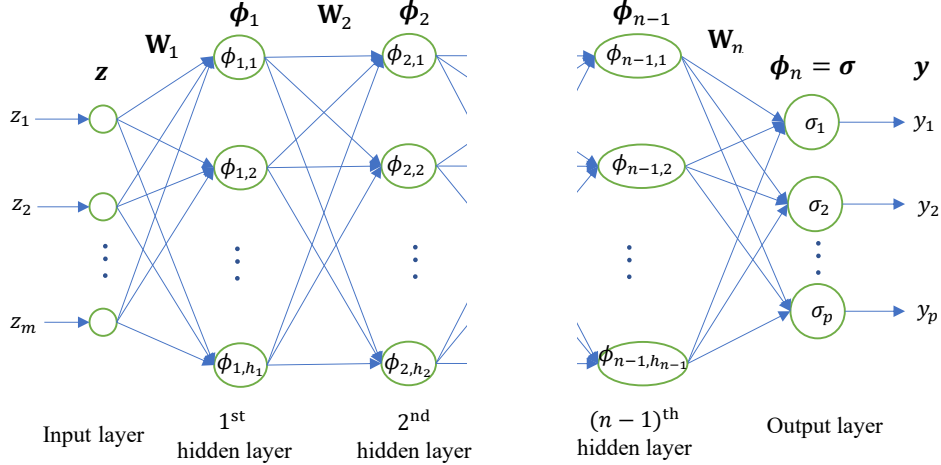


Figure 1: Structure of an n -layer feedforward neural network with input \mathbf{z} and target output \mathbf{y} .

According to the universal approximation theorem of neural networks [2, 3], the networks can approximate any function at any accuracy with sufficiently large number of hidden neurons.

3 Inverse Layer-wise Learning of Multilayer Feedforward Neural Networks

In this approach, the MLFN is trained layer-by-layer to ensure the convergence, which means one layer of weights is learned at a time. In [28], by using functional inverse and matrix pseudoinverse, equation (2) has been treated as follows with $\mathbf{y}_{\mathcal{N}\mathcal{N}} = \mathbf{y}$

$$\mathbf{y} = \phi_n(\mathbf{W}_n \phi_{n-1}(\mathbf{W}_{n-1} \phi_{n-2}(\dots \mathbf{W}_3 \phi_2(\mathbf{W}_2 \phi_1(\mathbf{W}_1 \mathbf{z})))) \quad (5)$$

$$\rightarrow \mathbf{W}_n^\dagger \phi_n^{-1}(\mathbf{y}) = \phi_{n-1}(\mathbf{W}_{n-1} \phi_{n-2}(\dots \mathbf{W}_3 \phi_2(\mathbf{W}_2 \phi_1(\mathbf{W}_1 \mathbf{z})))) \quad (6)$$

\vdots

$$\rightarrow \mathbf{W}_2^\dagger \phi_2^{-1}(\dots \mathbf{W}_{n-1}^\dagger \phi_{n-1}^{-1}(\mathbf{W}_n^\dagger \phi_n^{-1}(\mathbf{y}))) = \phi_1(\mathbf{W}_1 \mathbf{z}) \quad (7)$$

where $\mathbf{W}_n^\dagger, \mathbf{W}_{n-1}^\dagger, \dots, \mathbf{W}_2^\dagger$ are the Moore-Penrose inverses (or pseudoinverses) of matrices $\mathbf{W}_n, \mathbf{W}_{n-1}, \dots, \mathbf{W}_2$ respectively; $\phi_n^{-1}, \phi_{n-1}^{-1}, \dots, \phi_2^{-1}$ are vectors of inverse functions of respective $\phi_n, \phi_{n-1}, \dots, \phi_2$.

The inverse layer-wise learning is conducted through two stages in sequence: backward and forward. The learning process starts with the backward stage (subsection 3.1), where the MLFN is trained layer-wisely from the output layer to the input layer. After that, the forward stage takes place (subsection 3.2), where the network is trained layer-wisely in the forward direction, from the input layer to the output layer. Unlike in [28] where the author used the kernel and range space to solve linear equations, we propose nonlinear update laws to find the weight matrices incrementally so that the convergence is ensured.

3.1 Backward Stage of Inverse Layer-wise Learning

In the first stage of inverse layer-wise learning, the network is trained layer-by-layer from \mathbf{W}_n to \mathbf{W}_1 . That is, \mathbf{W}_n is trained first. Then comes $\mathbf{W}_{n-1}, \mathbf{W}_{n-2}, \dots$. The backward stage ends with the learning of the input weights \mathbf{W}_1 . Let us now look into the details of how the weights in each layer are trained, starting from \mathbf{W}_n . Prior to that, all the weight matrices $\mathbf{W}_1, \mathbf{W}_2, \dots, \mathbf{W}_{n-1}, \mathbf{W}_n$ are first randomly initialized. Let $\bar{\mathbf{W}}_1^*, \bar{\mathbf{W}}_2^*, \dots, \bar{\mathbf{W}}_{n-1}^*, \bar{\mathbf{W}}_n^*$ be the respective values of these matrices after initialization.

3.1.1 Learning of the output weights \mathbf{W}_n

During learning of \mathbf{W}_n (or the n^{th} layer), the other weight matrices are frozen at their initialized values $\bar{\mathbf{W}}_1^*, \bar{\mathbf{W}}_2^*, \dots, \bar{\mathbf{W}}_{n-1}^*$. Using these values, we can compute the input of the n^{th} layer, which is also the output after the $(n-1)^{\text{th}}$ hidden layer, by using (4)

$$\bar{\phi}_{n-1}^* = \phi_{n-1}(\bar{\mathbf{W}}_{n-1}^* \phi_{n-2}(\dots \phi_2(\bar{\mathbf{W}}_2^* \phi_1(\bar{\mathbf{W}}_1^* \mathbf{z})) \dots)) \quad (8)$$

Hence, the output of this n^{th} layer (and also of the whole MLFN), denoted as $\mathbf{y}_{\mathcal{NN}n}$, is given as

$$\mathbf{y}_{\mathcal{NN}n}(\mathbf{W}_n, \bar{\phi}_{n-1}^*) = \phi_n(\mathbf{W}_n \bar{\phi}_{n-1}^*) \quad (9)$$

This is actually equal to the right-hand side of (5) when setting $\mathbf{W}_1, \dots, \mathbf{W}_{n-1}$ as $\bar{\mathbf{W}}_1^*, \dots, \bar{\mathbf{W}}_{n-1}^*$, respectively. Hence, the target for learning of \mathbf{W}_n , denoted as \mathbf{y}_n , is the direct target \mathbf{y} of the whole MLFN as seen on the left-hand side of (5). That is

$$\mathbf{y}_n = \mathbf{y} \quad (10)$$

Given $\bar{\mathbf{W}}_1^*, \bar{\mathbf{W}}_2^*, \dots, \bar{\mathbf{W}}_{n-1}^*$, there exists a weight matrix \mathbf{W}_n such that the target provided in (10) can be approximated by the network whose output is given in (9). This is feasible if the number of neurons h_{n-1} is sufficiently large. We have

$$\mathbf{y}_n = \mathbf{y}_{\mathcal{NN}n}(\mathbf{W}_n, \bar{\phi}_{n-1}^*) = \phi_n(\mathbf{W}_n \bar{\phi}_{n-1}^*) \quad (11)$$

For learning of \mathbf{W}_n , an incremental learning update law, referred to as *one-layer update*, is developed to update the weights at that layer. In this algorithm, the weights in matrix \mathbf{W}_n are updated incrementally without inverting the activation functions in ϕ_n (and hence the update law is also called *nonlinear*). In each step of training, we use one example of the training data. At the k^{th} step, $(\mathbf{z}(k), \mathbf{y}(k))$ are used, and the target for training \mathbf{W}_n in (10) is given as

$$\mathbf{y}_n(k) = \mathbf{y}(k) \quad (12)$$

Equation (11) can be rewritten as

$$\mathbf{y}_n(k) = \mathbf{y}_{\mathcal{NN}n}(\mathbf{W}_n, \bar{\phi}_{n-1}^*(k)) = \phi_n(\mathbf{W}_n \bar{\phi}_{n-1}^*(k)) \quad (13)$$

$$\text{where } \bar{\phi}_{n-1}^*(k) = \phi_{n-1}(\bar{\mathbf{W}}_{n-1}^* \phi_{n-2}(\dots \phi_2(\bar{\mathbf{W}}_2^* \phi_1(\bar{\mathbf{W}}_1^* \mathbf{z}(k))) \dots)) \quad (14)$$

Let $\hat{\mathbf{W}}_n(k)$ denote the estimated weight matrix at the k^{th} step of training, the estimated output $\hat{\mathbf{y}}_n(k)$ at this k^{th} step is constructed as the direct output of this n^{th} layer when its weight matrix is set at $\hat{\mathbf{W}}_n(k)$:

$$\hat{\mathbf{y}}_n(k) = \mathbf{y}_{\mathcal{NN}n}(\hat{\mathbf{W}}_n(k), \bar{\boldsymbol{\phi}}_{n-1}^*(k)) = \phi_n(\hat{\mathbf{W}}_n(k) \bar{\boldsymbol{\phi}}_{n-1}^*(k)) \quad (15)$$

The output estimation error in learning of \mathbf{W}_n at the k^{th} step is defined as $\mathbf{e}_n(k) = \mathbf{y}_n(k) - \hat{\mathbf{y}}_n(k)$. Hence, from (13) and (15) we have

$$\mathbf{e}_n(k) = \mathbf{y}_{\mathcal{NN}n}(\mathbf{W}_n, \bar{\boldsymbol{\phi}}_{n-1}^*(k)) - \mathbf{y}_{\mathcal{NN}n}(\hat{\mathbf{W}}_n(k), \bar{\boldsymbol{\phi}}_{n-1}^*(k)) \quad (16)$$

$$\text{or } \mathbf{e}_n(k) = \phi_n(\mathbf{W}_n \bar{\boldsymbol{\phi}}_{n-1}^*(k)) - \phi_n(\hat{\mathbf{W}}_n(k) \bar{\boldsymbol{\phi}}_{n-1}^*(k)) \quad (17)$$

$$\text{Let } \boldsymbol{\delta}_n(k) \triangleq \mathbf{W}_n \bar{\boldsymbol{\phi}}_{n-1}^*(k) - \hat{\mathbf{W}}_n(k) \bar{\boldsymbol{\phi}}_{n-1}^*(k) = \Delta \mathbf{W}_n(k) \bar{\boldsymbol{\phi}}_{n-1}^*(k) \quad (18)$$

where $\Delta \mathbf{W}_n(k) = \mathbf{W}_n - \hat{\mathbf{W}}_n(k)$.

Let us consider the relationship between $\mathbf{e}_n(k)$ and $\boldsymbol{\delta}_n(k)$: If ϕ_n is chosen as a vector of monotonically increasing activation functions whose derivatives are bounded by f_{ϕ_n} , we have

- i, The corresponding elements of two vectors $\mathbf{e}_n(k)$ and $\boldsymbol{\delta}_n(k)$ have the same sign, i.e.

$$e_{n,i}(k) \delta_{n,i}(k) \geq 0, \forall i = 1..h_n \quad (19)$$

- ii, The absolute value of an element of $\mathbf{e}_n(k)$ is less than or equal to f_{ϕ_n} times the corresponding element of $\boldsymbol{\delta}_n(k)$ i.e.

$$|e_{n,i}(k)| \leq f_{\phi_n} |\delta_{n,i}(k)|, \forall i = 1..h_n \quad (20)$$

The incremental learning law (one-layer update) to update the estimated weights based on the output estimation error is proposed as

$$\hat{\mathbf{W}}_n(k+1) = \hat{\mathbf{W}}_n(k) + \mathbf{L}_n(k) \mathbf{e}_n(k) \bar{\boldsymbol{\phi}}_{n-1}^{*T}(k) \quad (21)$$

where $\mathbf{L}_n(k) \in \mathbb{R}^{h_n \times h_n}$ is a positive diagonal matrix; $\bar{\boldsymbol{\phi}}_{n-1}^*(k)$ is calculated using (14); $\mathbf{e}_n(k) = \mathbf{y}_n(k) - \hat{\mathbf{y}}_n(k)$ with $\mathbf{y}_n(k)$ and $\hat{\mathbf{y}}_n(k)$ given in (12) and (15), respectively. Denoting $\mathbf{w}_{n,i}$ as the i^{th} column vector of matrix \mathbf{W}_n , $\hat{\mathbf{w}}_{n,i}(k)$ the i^{th} column vector of $\hat{\mathbf{W}}_n(k)$ and $\bar{\phi}_{n-1,i}^*(k)$ the i^{th} element of vector $\bar{\boldsymbol{\phi}}_{n-1}^*(k)$, the update law (21) can be rewritten in the vector form as

$$\hat{\mathbf{w}}_{n,i}(k+1) = \hat{\mathbf{w}}_{n,i}(k) + \bar{\phi}_{n-1,i}^*(k) \mathbf{L}_n(k) \mathbf{e}_n(k) \quad (22)$$

To show the convergence, we define an objective function as

$$V(k) = \sum_{i=1}^{h_n-1} \Delta \mathbf{w}_{n,i}^T(k) \Delta \mathbf{w}_{n,i}(k) \quad (23)$$

where $\Delta \mathbf{w}_{n,i}(k) = \mathbf{w}_{n,i} - \hat{\mathbf{w}}_{n,i}(k)$. The objective function at the $(k+1)^{\text{th}}$ step is

$$\begin{aligned} V(k+1) &= \sum_{i=1}^{h_{n-1}} \Delta \mathbf{w}_{n,i}^T(k+1) \Delta \mathbf{w}_{n,i}(k+1) \\ &= \sum_{i=1}^{h_{n-1}} (\Delta \mathbf{w}_{n,i}(k) - \bar{\phi}_{n-1,i}^*(k) \mathbf{L}_n(k) \mathbf{e}_n(k))^T \\ &\quad (\Delta \mathbf{w}_{n,i}(k) - \bar{\phi}_{n-1,i}^*(k) \mathbf{L}_n(k) \mathbf{e}_n(k)) \end{aligned} \quad (24)$$

A change of the objective function value when the learning step goes from k^{th} to $(k+1)^{\text{th}}$

$$\begin{aligned} \Delta V(k) &= V(k+1) - V(k) \\ &= \sum_{i=1}^{h_{n-1}} \left(-\bar{\phi}_{n-1,i}^*(k) \Delta \mathbf{w}_{n,i}^T(k) \mathbf{L}_n(k) \mathbf{e}_n(k) \right. \\ &\quad \left. - \bar{\phi}_{n-1,i}^*(k) \mathbf{e}_n^T(k) \mathbf{L}_n^T(k) \Delta \mathbf{w}_{n,i}(k) \right. \\ &\quad \left. + \bar{\phi}_{n-1,i}^{*2}(k) \mathbf{e}_n^T(k) \mathbf{L}_n^T(k) \mathbf{L}_n(k) \mathbf{e}_n(k) \right) \end{aligned} \quad (25)$$

From (18), we have $\boldsymbol{\delta}_n(k) = \Delta \mathbf{W}_n(k) \bar{\boldsymbol{\phi}}_{n-1}^*(k) = \sum_{i=1}^{h_{n-1}} \Delta \mathbf{w}_{n,i}(k) \bar{\phi}_{n-1,i}^*(k)$, hence

$$\begin{aligned} \Delta V(k) &= -\boldsymbol{\delta}_n^T(k) \mathbf{L}_n(k) \mathbf{e}_n(k) - \mathbf{e}_n^T(k) \mathbf{L}_n^T(k) \boldsymbol{\delta}_n(k) \\ &\quad + \sum_{i=1}^{h_{n-1}} \left(\bar{\phi}_{n-1,i}^{*2}(k) \mathbf{e}_n^T(k) \mathbf{L}_n^T(k) \mathbf{L}_n(k) \mathbf{e}_n(k) \right) \end{aligned} \quad (26)$$

From the properties stated in (19), (20), we have the following inequality since $\mathbf{L}_n(k)$ is a positive diagonal matrix

$$\boldsymbol{\delta}_n^T(k) \mathbf{L}_n(k) \mathbf{e}_n(k) \geq \frac{1}{f_{\phi_n}} \mathbf{e}_n^T(k) \mathbf{L}_n(k) \mathbf{e}_n(k) \quad (27)$$

which finally gives

$$\Delta V(k) \leq -\mathbf{e}_n^T(k) \left(\frac{2}{f_{\phi_n}} \mathbf{L}_n(k) - \sum_{i=1}^{h_{n-1}} \bar{\phi}_{n-1,i}^{*2}(k) \mathbf{L}_n^T(k) \mathbf{L}_n(k) \right) \mathbf{e}_n(k) \quad (28)$$

When $\mathbf{L}_n(k)$ is chosen such that

$$\frac{2}{f_{\phi_n}} \mathbf{L}_n(k) - \sum_{i=1}^{h_{n-1}} \bar{\phi}_{n-1,i}^{*2}(k) \mathbf{L}_n^T(k) \mathbf{L}_n(k) > 0 \quad (29)$$

then $\Delta V(k)$ is negative if $\mathbf{e}_n(k)$ is non-zero. That means, the value of objective function keeps decreasing $V(k+1) < V(k)$. Moreover, since the function $V(k)$ is non-negative, which means it is bounded from below, we have $\Delta V(k)$ converges as k increases. Thus, from (28), $\mathbf{e}_n(k)$ converges as k increases.

3.1.2 Learning of the hidden weights \mathbf{W}_j with $n-1 \geq j \geq 2$

After \mathbf{W}_n has been learned and its value in this backward stage has been obtained as $\bar{\mathbf{W}}_n^b$, the target for the $(n-1)^{\text{th}}$ layer is calculated based on the left hand side of (6) as $\mathbf{y}_{n-1} = \bar{\mathbf{W}}_n^{b\dagger} \phi_n^{-1}(\mathbf{y}_n)$. Generally, the target for learning of \mathbf{W}_j (or the j^{th} layer), denoted as \mathbf{y}_j , can be achieved by calculating backwardly from the target for the last layer $\mathbf{y}_n = \mathbf{y}$, using the left-hand sides of equations from (5) to (7). We have

$$\mathbf{y}_j = \bar{\mathbf{W}}_{j+1}^{b\dagger} \phi_{j+1}^{-1}(\mathbf{y}_{j+1}) \text{ with } n-1 \geq j \geq 1 \quad (30)$$

A graphical illustration of the backward calculation of the target is shown in Fig. 2.

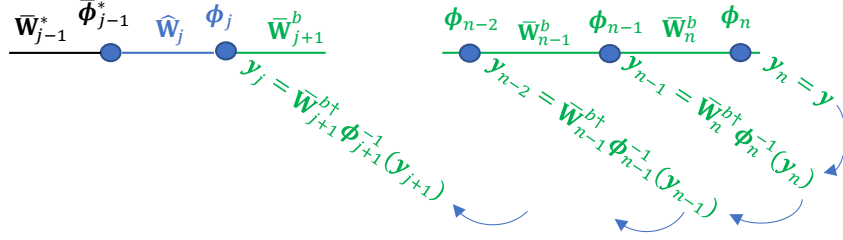


Figure 2: Backward transmission of the target in inverse layer-wise learning, from the output layer to the inner layers.

The input of the j^{th} layer is computed similarly to (8) using (4)

$$\bar{\phi}_{j-1}^* \triangleq \phi_{j-1}(\bar{\mathbf{W}}_{j-1}^* \phi_{j-2}(\dots \phi_2(\bar{\mathbf{W}}_2^* \phi_1(\bar{\mathbf{W}}_1^* \mathbf{z}))) \dots)) \quad (31)$$

Hence, the output of this j^{th} layer is given as

$$\mathbf{y}_{\mathcal{NN}j}(\mathbf{W}_j, \bar{\phi}_{j-1}^*) = \phi_j(\mathbf{W}_j \bar{\phi}_{j-1}^*) \quad (32)$$

There exists a weight matrix \mathbf{W}_j such that the target provided in (30) can be approximated by the network whose output is given in (32)

$$\mathbf{y}_j = \mathbf{y}_{\mathcal{NN}j}(\mathbf{W}_j, \bar{\phi}_{j-1}^*) = \phi_j(\mathbf{W}_j \bar{\phi}_{j-1}^*) \quad (33)$$

Similar to learning of \mathbf{W}_n , the weights in matrix \mathbf{W}_j are updated incrementally without inverting the activation functions ϕ_j . The functions ϕ_j are chosen to be monotonically increasing activation functions and their derivatives are bounded by f_{ϕ_j} . At the k^{th} step of training, equation (30) can be rewritten as

$$\mathbf{y}_j(k) = \bar{\mathbf{W}}_{j+1}^{b\dagger} \phi_{j+1}^{-1}(\mathbf{y}_{j+1}(k)) \quad (34)$$

and equation (33) can be rewritten as

$$\mathbf{y}_j(k) = \mathbf{y}_{\mathcal{NN}j}(\mathbf{W}_j, \bar{\phi}_{j-1}^*(k)) = \phi_j(\mathbf{W}_j \bar{\phi}_{j-1}^*(k)) \quad (35)$$

$$\text{where } \bar{\phi}_{j-1}^*(k) = \phi_{j-1}(\bar{\mathbf{W}}_{j-1}^* \phi_{j-2}(\dots \phi_2(\bar{\mathbf{W}}_2^* \phi_1(\bar{\mathbf{W}}_1^* \mathbf{z}(k)))) \dots)) \quad (36)$$

Let $\hat{\mathbf{W}}_j(k)$ denote the estimated weight matrix at the k^{th} step of training, the estimated output $\hat{\mathbf{y}}_j(k)$ at the k^{th} step is constructed as the direct output of this j^{th} layer when its weight matrix is set at $\hat{\mathbf{W}}_j(k)$:

$$\hat{\mathbf{y}}_j(k) = \mathbf{y}_{\mathcal{NN}j}(\hat{\mathbf{W}}_j(k), \bar{\boldsymbol{\phi}}_{j-1}^*(k)) = \boldsymbol{\phi}_j(\hat{\mathbf{W}}_j(k) \bar{\boldsymbol{\phi}}_{j-1}^*(k)) \quad (37)$$

The output estimation error in learning of \mathbf{W}_j at the k^{th} step is defined as $\mathbf{e}_j(k) = \mathbf{y}_j(k) - \hat{\mathbf{y}}_j(k)$. Hence,

$$\mathbf{e}_j(k) = \mathbf{y}_{\mathcal{NN}j}(\mathbf{W}_j, \bar{\boldsymbol{\phi}}_{j-1}^*(k)) - \mathbf{y}_{\mathcal{NN}j}(\hat{\mathbf{W}}_j(k), \bar{\boldsymbol{\phi}}_{j-1}^*(k)) \quad (38)$$

The incremental learning law to update the estimated weights based on the output estimation error is proposed as

$$\hat{\mathbf{W}}_j(k+1) = \hat{\mathbf{W}}_j(k) + \mathbf{L}_j(k) \mathbf{e}_j(k) \bar{\boldsymbol{\phi}}_{j-1}^{*T}(k) \quad (39)$$

where $\mathbf{L}_j(k) \in \mathbb{R}^{h_j \times h_j}$ is a positive diagonal matrix that satisfies the following condition

$$\frac{2}{f_{\phi_j}} \mathbf{L}_j(k) - \sum_{i=1}^{h_{j-1}} \bar{\phi}_{j-1,i}^{*2}(k) \mathbf{L}_j^T(k) \mathbf{L}_j(k) > 0 \quad (40)$$

with $\bar{\phi}_{j-1,i}^{*2}(k)$ being the i^{th} element of vector $\bar{\boldsymbol{\phi}}_{j-1}^*(k)$; $\bar{\boldsymbol{\phi}}_{j-1}^*(k)$ is calculated using (36); $\mathbf{e}_j(k) = \mathbf{y}_j(k) - \hat{\mathbf{y}}_j(k)$ with $\mathbf{y}_j(k)$ and $\hat{\mathbf{y}}_j(k)$ given in (34) and (37), respectively.

Similarly to the case of \mathbf{W}_n , it can be shown that $\mathbf{e}_j(k)$ converges as k increases.

3.1.3 Learning of the input weights \mathbf{W}_1

Learning of \mathbf{W}_1 is done in the same way as learning of \mathbf{W}_j above by setting $j = 1$. One point to take note is that the denotations of $\bar{\boldsymbol{\phi}}_{j-1}^*$ and h_{j-1} in above demonstration would become $\bar{\boldsymbol{\phi}}_0^*$ and h_0 which do not exist. However, it is possible to consider that $\bar{\boldsymbol{\phi}}_0^* \triangleq \mathbf{z}$ ($\bar{\phi}_{0,i}^* \triangleq z_i$) and $h_0 \triangleq m$ (m is the dimension of the input vector \mathbf{z}). After learning, we get $\bar{\mathbf{W}}_1^b$. The backward stage stops.

3.2 Forward Stage of Inverse Layer-wise Learning

In the forward stage, the network is trained forwardly from the input layer to the output layer. The inverse layer-wise learning goes forwards from \mathbf{W}_2 until the output weights \mathbf{W}_n are retrained.

In this stage, the learning can be conducted similarly for every layer from \mathbf{W}_2 to \mathbf{W}_n . The only difference is that in the backward stage, the input of the j^{th} layer was defined based on the initialized values of $\bar{\mathbf{W}}_1^*, \bar{\mathbf{W}}_2^*, \dots, \bar{\mathbf{W}}_{j-1}^*$ as in (31), but it is now defined based on the values of weights $\bar{\mathbf{W}}_1, \bar{\mathbf{W}}_2, \dots, \bar{\mathbf{W}}_{j-1}$ that have been relearned before \mathbf{W}_j

$$\bar{\boldsymbol{\phi}}_{j-1} = \boldsymbol{\phi}_{j-1}(\bar{\mathbf{W}}_{j-1} \boldsymbol{\phi}_{j-2}(\dots \boldsymbol{\phi}_2(\bar{\mathbf{W}}_2 \boldsymbol{\phi}_1(\bar{\mathbf{W}}_1 \mathbf{z})) \dots)) \quad \text{with } 2 \leq j \leq n \quad (41)$$

with noting that $\bar{\mathbf{W}}_1 = \bar{\mathbf{W}}_1^b$ since there is no forward learning for \mathbf{W}_1 .

3.3 The Step-by-Step Algorithm

This part summarizes the inverse layer-wise learning of MLFNs. In each layer, the weights are updated incrementally by a one-layer update law. The details of the inverse layer-wise learning algorithm are as follows

- (i) Initialization: Randomly assign $\mathbf{W}_1, \mathbf{W}_2, \dots, \mathbf{W}_n$.
- (ii) Train \mathbf{W}_n using update law (21) \rightarrow obtain $\bar{\mathbf{W}}_n^b$
- (iii) Backward looping: Learning of \mathbf{W}_j (from \mathbf{W}_{n-1} to \mathbf{W}_1)
 - (a) Set $j = n - 1$
 - (b) Train \mathbf{W}_j using update law (39) \rightarrow obtain $\bar{\mathbf{W}}_j^b$
 - (c) Decrease j by 1 and go to step (b) if $j \geq 1$
- (iv) Forward looping: Learning of \mathbf{W}_j again (from \mathbf{W}_2 to \mathbf{W}_n)
 - (d) Set $j = 2$
 - (e) Train \mathbf{W}_j using update law (39) with noting that $\bar{\phi}_{j-1}$ in (41) is used instead of $\bar{\phi}_{j-1}^*$ \rightarrow obtain $\bar{\mathbf{W}}_j$
 - (f) Increase j by 1 and go to step (e) if $j \leq n$

In learning of each layer, the number of training steps can exceed the number of training examples. This is because after all the examples in the training data have been used, the full training set can be used again. Each time when a full set of training data is used is called a loop. In practice, the training of each layer can take many loops.

3.4 Classification on MNIST Database and Performance Issue of Inverse Layer-wise Learning

MNIST database was used for assessing the performance of the inverse layer-wise learning algorithm to understand the issues associated with it.

3.4.1 Network structure and learning results

The network built has the following properties:

- A 3-hidden layer network with structure 784-300-100-50-10 (300 units, 100 units, and 50 units in hidden layers). The activation functions at hidden layers are modified softplus $f(x) = \log(0.8 + e^x)$ as suggested in [28], which has its inverse function as $\log(e^x - 0.8)$. The activation functions at output is sigmoid $f(x) = 1/(1 + e^{-x})$.

In this network, there are 4 weight matrices to be learned: $\mathbf{W}_1, \mathbf{W}_2, \mathbf{W}_3$ and \mathbf{W}_4 . Before training all of the weights, \mathbf{W}_1 to \mathbf{W}_4 were randomly initialized. After that, learning process began with learning of $\mathbf{W}_4 \rightarrow$ learning of $\mathbf{W}_3 \rightarrow$ learning of $\mathbf{W}_2 \rightarrow$ learning of $\mathbf{W}_1 \rightarrow$ relearning of $\mathbf{W}_2 \rightarrow$ relearning of $\mathbf{W}_3 \rightarrow$ relearning of \mathbf{W}_4 . In learning of each layer, the gain matrix \mathbf{L} was not a predefined matrix. Instead, it was calculated from the respective conditions in (29) and (40) to ensure the convergence of the learning process. Since the matrix is diagonal and the inequalities are quite straightforward, the gain matrix \mathbf{L} can be directly calculated. The number of loops for training of each layer was 20.

The results in Table 1 show that although convergence can be achieved, the accuracy after training by inverse layer-wise learning algorithm is not desirable as compared to the stochastic gradient descent (SGD) method (92.04% compared to 98.36% on the test set). Noting that for the

Table 1: Training & testing accuracies (%) by inverse layer-wise learning vs. SGD

	Training	Testing
Inverse layer-wise learning	92.37	92.04
Stochastic gradient descent	99.80	98.36

purpose of comparing with the best performance, the results for SGD method in this paper were achieved by observing the accuracy directly on the test set while training and no validation set was used.

3.4.2 Discussions on the results of inverse layer-wise learning

The inverse layer-wise learning method is non-error-based, which means that the error at the output layer of the MLFN is not directly used to adjust all layers of weights (the output error is only used directly for training the last layer). Instead, the target is transmitted backwards to previous layers in a backward transmission process (please refer to (30) and Fig. 2). Though convergence can now be ensured in leaning, this backward transmission of target causes some possible problems that lead to a trade off in accuracy as compared to backpropagation (like SGD) method. One of the reasons can stem from the fact that the modified softplus and sigmoid are only invertible within their ranges. This causes the distortions in the target values when transmitted backwardly. Even when all the nonlinear functions are fully invertible and the targets for previous layer are right values, training only a layer of weights may not help in fitting the target for that layer. Therefore the inverse layer-wise learning method can be used in cases where a trade off in performance is acceptable while ensuring the convergence of the learning systems. In the next section, we present a learning method to achieve a good balance between accuracy and convergence.

4 Forward Progressive Learning of Multilayer Feedforward Neural Networks

In this section, we develop a forward progressive leaning (FPL) method based on the layer-wise methodology referred in [30–32]. Unlike those works [30–32] where there is no convergence analysis, the convergence can be analyzed in our proposed FPL method. Our main aim here is to develop an output-error-based layer-wise learning algorithm so as to overcome the drawback of the inverse layer-wise leaning method in section 3.

Fig. 3 illustrates the processing details of the algorithms. The overall structure of the deep network with n weight matrices to be learned is shown in Fig 3(a). The FPL starts with learning of the weights in the first layer \mathbf{W}_1 based on an SLFN (or two-layer network) where the first hidden layer is directly connected to the output, as shown in fig 3(b). Two weight matrices, an input weight matrix \mathbf{W}_1 and a pseudo output weight matrix $\mathbf{W}_1^\triangleright$, are learned simultaneously by a two-layer algorithm. After learning, the matrix $\bar{\mathbf{W}}_1$ is kept to form new input for the next layer while the pseudo output weight matrix $\bar{\mathbf{W}}_1^\triangleright$ is discarded. Fig 3(c) shows the learning of the second layer \mathbf{W}_2 based on a second SLFN with two weight matrices \mathbf{W}_2 and $\mathbf{W}_2^\triangleright$. New input \mathbf{z}_2 of this SLFN has been formed by passing \mathbf{z} through fixed $\bar{\mathbf{W}}_1$. Similarly, after training we keep $\bar{\mathbf{W}}_2$ and discard $\bar{\mathbf{W}}_2^\triangleright$. Fig 3(d) shows the learning of the j^{th} layer \mathbf{W}_j with input \mathbf{z}_j and target output \mathbf{y} .

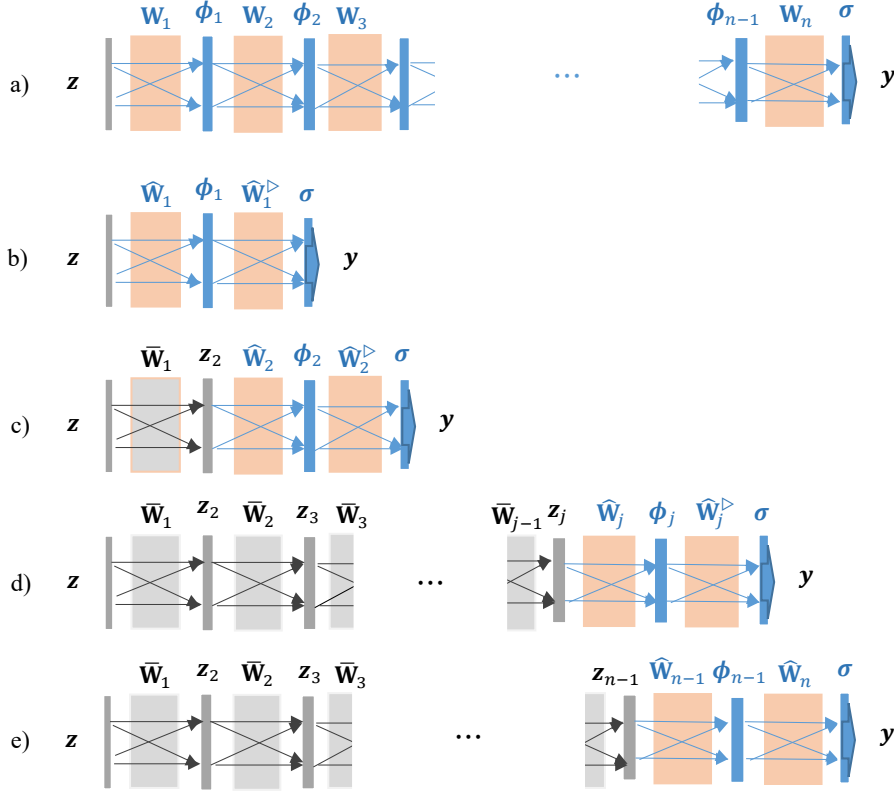


Figure 3: Forward progressive learning (FPL) method, where an n -layer network is trained layer-wisely through learning of $(n-1)$ two-layer networks. Each two-layer network is trained in 2 phases: pre-training (subsection 4.1) and fine-tuning (subsection 4.2) so as to guarantee the convergence.

The FPL continues until the learning of \mathbf{W}_{n-1} takes place as shown in Fig 3(e), where the pseudo output weights are no longer needed. Instead, the true output weights of the deep net \mathbf{W}_n is used and trained together with \mathbf{W}_{n-1} . After training this SLFN, the FPL ends.

We now consider a general case when the j^{th} hidden layer is added. The structure of the SLFN in this case is shown in Fig. 4. Since $\bar{\mathbf{W}}_1, \dots, \bar{\mathbf{W}}_{j-1}$ have been trained, the input to this SLFN can be calculated similarly to (31)

$$\mathbf{z}_j \triangleq \bar{\phi}_{j-1} = \phi_{j-1}(\bar{\mathbf{W}}_{j-1} \phi_{j-2}(\dots \phi_2(\bar{\mathbf{W}}_2 \phi_1(\bar{\mathbf{W}}_1 \mathbf{z})) \dots)) \quad (42)$$

The output of the network as shown in Fig. 4 can be expressed as follows:

$$\mathbf{y}_{\mathcal{NN}}(\mathbf{W}_j, \mathbf{W}_j^{\triangleright}, \mathbf{z}_j) = \sigma(\mathbf{W}_j^{\triangleright} \phi_j(\mathbf{W}_j \mathbf{z}_j)) \quad (43)$$

Each SLFN is trained in two phases. In the first phase, called pre-training, the proposed one-layer update law in section 3 is adopted to pre-train the SLFN. In the second phase, called fine-tuning, a two-layer update law is developed to fine-tune the weights of the SLFN.

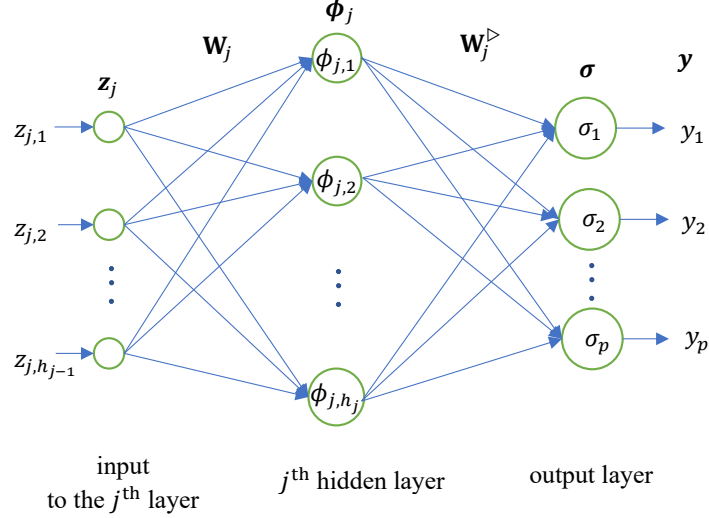


Figure 4: The single hidden layer feedforward network (or two-layer network) for new added j^{th} hidden layer in forward progressive learning. The input \mathbf{z}_j of this network is calculated by forwardly propagating \mathbf{z} through previous layers which have been learned, while its target is the overall target \mathbf{y} directly.

4.1 Pre-training of Single Hidden Layer Feedforward Networks

The purpose of the pre-training phase is to achieve a sufficiently small estimation error, before further improvement is achieved by a fine-tuning phase.

The proposed one-layer update law for training the last layer of an MLFN is used to pre-train the SLFN. The steps of training are as follows:

- Initialization: Randomly assign \mathbf{W}_j and \mathbf{W}_j^D to $\bar{\mathbf{W}}_j^*$ and $\bar{\mathbf{W}}_j^{D*}$ respectively.
- \mathbf{W}_j^D is trained using update law (21) to obtain $\bar{\mathbf{W}}_j^D$.

After \mathbf{W}_j^D has been pre-trained, the entire SLFN will be trained one more time in a fine-tuning phase.

Noting that the inverse layer-wise algorithm presented in the previous section can also be used to achieved this aim.

4.2 Fine-Tuning of Single Hidden Layer Feedforward Networks

In this subsection, a *two-layer update* law is developed to update concurrently both the input weights \mathbf{W}_j and the output weights \mathbf{W}_j^D of the SLFN. When the number of neurons in the hidden layer h_j is sufficiently large, there exist weight matrices \mathbf{W}_j and \mathbf{W}_j^D such that the target provided in (1) can be approximated by the network whose output is given in (43)

$$\mathbf{y}(k) = \mathbf{y}_{\mathcal{NN}}(\mathbf{W}_j, \mathbf{W}_j^D, \mathbf{z}_j(k)) = \boldsymbol{\sigma}(\mathbf{W}_j^D \boldsymbol{\phi}_j(\mathbf{W}_j \mathbf{z}_j(k))) \quad (44)$$

As \mathbf{W}_j and \mathbf{W}_j^D are unknown, they are updated incrementally by two learning laws. Let $\hat{\mathbf{W}}_j(k)$ and $\hat{\mathbf{W}}_j^D(k)$ denote the estimated weight matrices \mathbf{W}_j and \mathbf{W}_j^D at the k^{th} step of learning, the

estimated output vector $\hat{\mathbf{y}}(k)$ at the k^{th} step is constructed as the output of the SLFN when its weights are set at $\hat{\mathbf{W}}_j(k)$ and $\hat{\mathbf{W}}_j^{\triangleright}(k)$

$$\hat{\mathbf{y}}(k) = \mathbf{y}_{\mathcal{NN}}(\hat{\mathbf{W}}_j(k), \hat{\mathbf{W}}_j^{\triangleright}(k), \mathbf{z}_j(k)) = \boldsymbol{\sigma}(\hat{\mathbf{W}}_j^{\triangleright}(k)\boldsymbol{\phi}_j(\hat{\mathbf{W}}_j(k)\mathbf{z}_j(k))) \quad (45)$$

The output estimation error at the k^{th} step is defined as $\mathbf{e}(k) = \mathbf{y}(k) - \hat{\mathbf{y}}(k)$. Hence,

$$\mathbf{e}(k) = \mathbf{y}_{\mathcal{NN}}(\mathbf{W}_j, \mathbf{W}_j^{\triangleright}, \mathbf{z}_j(k)) - \mathbf{y}_{\mathcal{NN}}(\hat{\mathbf{W}}_j(k), \hat{\mathbf{W}}_j^{\triangleright}(k), \mathbf{z}_j(k)) \quad (46)$$

$$= \boldsymbol{\sigma}(\mathbf{W}_j^{\triangleright}\boldsymbol{\phi}_j(\mathbf{W}_j\mathbf{z}_j(k))) - \boldsymbol{\sigma}(\hat{\mathbf{W}}_j^{\triangleright}(k)\boldsymbol{\phi}_j(\hat{\mathbf{W}}_j(k)\mathbf{z}_j(k))) \quad (47)$$

Let

$$\boldsymbol{\delta}(k) \triangleq \mathbf{W}_j^{\triangleright}\boldsymbol{\phi}_j(\mathbf{W}_j\mathbf{z}_j(k)) - \hat{\mathbf{W}}_j^{\triangleright}(k)\boldsymbol{\phi}_j(\hat{\mathbf{W}}_j(k)\mathbf{z}_j(k)) \quad (48)$$

which can be expressed as

$$\boldsymbol{\delta}(k) = \hat{\mathbf{W}}_j^{\triangleright}(k)\Delta\boldsymbol{\phi}_j(k) + \Delta\mathbf{W}_j^{\triangleright}(k)\hat{\boldsymbol{\phi}}_j(k) + \Delta\mathbf{W}_j^{\triangleright}(k)\Delta\boldsymbol{\phi}_j(k) \quad (49)$$

where $\Delta\boldsymbol{\phi}_j(k) \triangleq \boldsymbol{\phi}_j(\mathbf{W}_j\mathbf{z}_j(k)) - \boldsymbol{\phi}_j(\hat{\mathbf{W}}_j(k)\mathbf{z}_j(k))$, $\hat{\boldsymbol{\phi}}_j(k) \triangleq \boldsymbol{\phi}_j(\hat{\mathbf{W}}_j(k)\mathbf{z}_j(k))$ and $\Delta\mathbf{W}_j^{\triangleright}(k) \triangleq \mathbf{W}_j^{\triangleright} - \hat{\mathbf{W}}_j^{\triangleright}(k)$.

Consequently, the incremental learning laws (two-layer update) to update the estimated weight based on the output estimation error $\mathbf{e}(k)$ are proposed as:

$$\hat{\mathbf{W}}_j^{\triangleright}(k+1) = \hat{\mathbf{W}}_j^{\triangleright}(k) + \alpha_1 \mathbf{L}(k)\mathbf{e}(k)\hat{\boldsymbol{\phi}}_j^T(k) \quad (50)$$

$$\hat{\mathbf{W}}_j(k+1) = \hat{\mathbf{W}}_j(k) + \alpha_0 \mathbf{P}(k)\mathbf{e}(k)\mathbf{z}_j^T(k) \quad (51)$$

where α_1 and α_0 are positive scalars, $\mathbf{L}(k) \in \mathbb{R}^{p \times p}$ is a positive diagonal matrix, $\mathbf{P}(k) \in \mathbb{R}^{h_j \times p}$ is a matrix depending on the learning step k .

In (50), let $\mathbf{w}_{j,i}^{\triangleright}$ denote the i^{th} column vector of matrix $\mathbf{W}_j^{\triangleright}$, $\hat{\mathbf{w}}_{j,i}^{\triangleright}(k)$ the i^{th} column vector of $\hat{\mathbf{W}}_j^{\triangleright}(k)$ and $\hat{\phi}_{j,i}(k)$ the i^{th} element of vector $\hat{\boldsymbol{\phi}}_j(k)$. In (51), let $\mathbf{w}_{j,i}$ denote the i^{th} column vector of matrix \mathbf{W}_j , $\hat{\mathbf{w}}_{j,i}(k)$ the i^{th} column vector of $\hat{\mathbf{W}}_j(k)$ and $z_{j,i}(k)$ the i^{th} element of the vector $\mathbf{z}_j(k)$. The update laws (50) and (51) can be rewritten in vector form as:

$$\hat{\mathbf{w}}_{j,i}^{\triangleright}(k+1) = \hat{\mathbf{w}}_{j,i}^{\triangleright}(k) + \alpha_1 \hat{\phi}_{j,i}(k)\mathbf{L}(k)\mathbf{e}(k) \quad (52)$$

$$\hat{\mathbf{w}}_{j,i}(k+1) = \hat{\mathbf{w}}_{j,i}(k) + \alpha_0 z_{j,i}(k)\mathbf{P}(k)\mathbf{e}(k) \quad (53)$$

To show the convergence, we define an objective function given by

$$V(k) = \frac{1}{\alpha_1} \sum_{i=1}^{h_j} \Delta\mathbf{w}_{j,i}^{\triangleright T}(k)\Delta\mathbf{w}_{j,i}^{\triangleright}(k) + \frac{1}{\alpha_0} \sum_{i=1}^{h_j-1} \Delta\mathbf{w}_{j,i}^T(k)\Delta\mathbf{w}_{j,i}(k) \quad (54)$$

where $\Delta\mathbf{w}_{j,i}^{\triangleright}(k) = \mathbf{w}_{j,i}^{\triangleright} - \hat{\mathbf{w}}_{j,i}^{\triangleright}(k)$ and $\Delta\mathbf{w}_{j,i}(k) = \mathbf{w}_{j,i} - \hat{\mathbf{w}}_{j,i}(k)$. From (52) and (53), the objective function at the $(k+1)^{\text{th}}$ step can be written as

$$V(k+1) = \frac{1}{\alpha_1} \sum_{i=1}^{h_j} \Delta\mathbf{w}_{j,i}^{\triangleright T}(k+1)\Delta\mathbf{w}_{j,i}^{\triangleright}(k+1) + \frac{1}{\alpha_0} \sum_{i=1}^{h_j-1} \Delta\mathbf{w}_{j,i}^T(k+1)\Delta\mathbf{w}_{j,i}(k+1)$$

Using (52) and (53), a change of the objective function value when the training step goes from k^{th} to $(k+1)^{\text{th}}$ can therefore be derived as

$$\begin{aligned}
\Delta V(k) &= V(k+1) - V(k) \\
&= -\hat{\phi}_j^T(k)\Delta\mathbf{W}_j^{\triangleright T}(k)\mathbf{L}(k)\mathbf{e}(k) - \mathbf{z}_j^T(k)\Delta\mathbf{W}_j^T(k)\mathbf{P}(k)\mathbf{e}(k) \\
&\quad - \mathbf{e}^T(k)\mathbf{L}^T(k)\Delta\mathbf{W}_j^{\triangleright}(k)\hat{\phi}_j(k) - \mathbf{e}^T(k)\mathbf{P}^T(k)\Delta\mathbf{W}_j(k)\mathbf{z}_j(k) \\
&\quad + \mathbf{e}^T(k)\left(\alpha_1\sum_{i=1}^{h_j}\hat{\phi}_{j,i}^2(k)\mathbf{L}^T(k)\mathbf{L}(k) + \alpha_0\sum_{i=1}^{h_{j-1}}z_{j,i}^2(k)\mathbf{P}^T(k)\mathbf{P}(k)\right)\mathbf{e}(k) \tag{55}
\end{aligned}$$

From (49), we have

$$\Delta\mathbf{W}_j^{\triangleright}(k)\hat{\phi}_j(k) = \boldsymbol{\delta}(k) - \hat{\mathbf{W}}_j^{\triangleright}(k)\Delta\phi_j(k) - \Delta\mathbf{W}_j^{\triangleright}(k)\Delta\phi_j(k) \tag{56}$$

Next, substituting into (55) gives

$$\begin{aligned}
\Delta V(k) &= -\boldsymbol{\delta}^T(k)\mathbf{L}(k)\mathbf{e}(k) - \mathbf{e}^T(k)\mathbf{L}^T(k)\boldsymbol{\delta}(k) \\
&\quad + \left(\Delta\phi_j^T(k)\hat{\mathbf{W}}_j^{\triangleright T}(k) - \mathbf{z}_j^T(k)\Delta\mathbf{W}_j^T(k)\mathbf{P}(k)\mathbf{L}^{-1}(k)\right)\mathbf{L}(k)\mathbf{e}(k) \\
&\quad + \mathbf{e}^T(k)\mathbf{L}^T(k)\left(\hat{\mathbf{W}}_j^{\triangleright}(k)\Delta\phi_j(k) - \mathbf{L}^{-T}(k)\mathbf{P}^T(k)\Delta\mathbf{W}_j(k)\mathbf{z}_j(k)\right) \\
&\quad + \mathbf{e}^T(k)\left(\alpha_1\sum_{i=1}^{h_j}\hat{\phi}_{j,i}^2(k)\mathbf{L}^T(k)\mathbf{L}(k) + \alpha_0\sum_{i=1}^{h_{j-1}}z_{j,i}^2(k)\mathbf{P}^T(k)\mathbf{P}(k)\right)\mathbf{e}(k) \\
&\quad + \Delta\phi_j^T(k)\Delta\mathbf{W}_j^{\triangleright T}(k)\mathbf{L}(k)\mathbf{e}(k) + \mathbf{e}^T(k)\mathbf{L}^T(k)\Delta\mathbf{W}_j^{\triangleright}(k)\Delta\phi_j(k) \tag{57}
\end{aligned}$$

After the pre-training phase, the errors are sufficiently small and hence the last two terms which are of O^3 are negligible as compared to the other terms which are of O^2 . Also, let the matrix $\mathbf{P}(k)$ be chosen so that $\boldsymbol{\xi}(k) \triangleq \hat{\mathbf{W}}_j^{\triangleright}(k)\Delta\phi_j(k) - \mathbf{L}^{-T}(k)\mathbf{P}^T(k)\Delta\mathbf{W}_j(k)\mathbf{z}_j(k)$ is zero or sufficiently small, then the equation (57) becomes

$$\begin{aligned}
\Delta V(k) &= -\boldsymbol{\delta}^T(k)\mathbf{L}(k)\mathbf{e}(k) - \mathbf{e}^T(k)\mathbf{L}^T(k)\boldsymbol{\delta}(k) \\
&\quad + \mathbf{e}^T(k)\left(\alpha_1\sum_{i=1}^{h_j}\hat{\phi}_{j,i}^2(k)\mathbf{L}^T(k)\mathbf{L}(k) + \alpha_0\sum_{i=1}^{h_{j-1}}z_{j,i}^2(k)\mathbf{P}^T(k)\mathbf{P}(k)\right)\mathbf{e}(k) \tag{58}
\end{aligned}$$

Similarly to the one-layer update, if the activation functions in σ are monotonically increasing and their derivatives are bounded by f_σ , comparing between $\mathbf{e}(k)$ in (47) and $\boldsymbol{\delta}(k)$ in (48), we have

i, The corresponding elements of $\mathbf{e}(k)$ and $\boldsymbol{\delta}(k)$ have the same sign, i.e.

$$e_i(k)\delta_i(k) \geq 0, \forall i = 1..p \tag{59}$$

ii, The absolute values of the elements of $\mathbf{e}(k)$ are less than or equal to f_σ times the corresponding elements of $\boldsymbol{\delta}(k)$ i.e.

$$|e_i(k)| \leq f_\sigma|\delta_i(k)|, \forall i = 1..p \tag{60}$$

From the properties stated in (59), (60), the following inequality can be assured

$$\begin{aligned} \Delta V(k) \leq & -\frac{2}{f_\sigma} \mathbf{e}^T(k) \mathbf{L}(k) \mathbf{e}(k) \\ & + \mathbf{e}^T(k) \left(\alpha_1 \sum_{i=1}^{h_j} \hat{\phi}_{j,i}^2(k) \mathbf{L}^T(k) \mathbf{L}(k) + \alpha_0 \sum_{i=1}^{h_{j-1}} z_{j,i}^2(k) \mathbf{P}^T(k) \mathbf{P}(k) \right) \mathbf{e}(k) \end{aligned} \quad (61)$$

When $\mathbf{L}(k)$ is chosen such that

$$\frac{2}{f_\sigma} \mathbf{L}(k) - \left(\alpha_1 \sum_{i=1}^{h_j} \hat{\phi}_{j,i}^2(k) \mathbf{L}^T(k) \mathbf{L}(k) + \alpha_0 \sum_{i=1}^{h_{j-1}} z_{j,i}^2(k) \mathbf{P}^T(k) \mathbf{P}(k) \right) > 0 \quad (62)$$

then $\Delta V(k)$ is negative if $\mathbf{e}(k)$ is non-zero. That means, the value of objective function keeps decreasing $V(k+1) < V(k)$. Moreover, since the function $V(k)$ is non-negative, which means it is bounded from below, we have $\Delta V(k)$ converges as k increases. Thus, from (61), $\mathbf{e}(k)$ converges as k increases.

However, to achieve

$$\boldsymbol{\xi}(k) = \hat{\mathbf{W}}_j^\triangleright(k) \Delta \boldsymbol{\phi}_j(k) - \mathbf{L}^{-T}(k) \mathbf{P}^T(k) \Delta \mathbf{W}_j(k) \mathbf{z}_j(k) \approx 0 \quad (63)$$

is not straightforward as it depends on the choices of $\boldsymbol{\phi}_j$. Let us now analyze the choice of $\mathbf{P}(k)$.

Discussions: Setting $\mathbf{P}(k) = \boldsymbol{\Theta}^T(k) \hat{\mathbf{W}}_j^{\triangleright T}(k) \mathbf{L}(k)$, where $\boldsymbol{\Theta}(k) \in \mathbb{R}^{h_j \times h_j}$, we have

$$\boldsymbol{\xi}(k) = \hat{\mathbf{W}}_j^\triangleright(k) (\Delta \boldsymbol{\phi}_j(k) - \boldsymbol{\Theta}(k) \Delta \mathbf{W}_j(k) \mathbf{z}_j(k)) \quad (64)$$

To achieve $\boldsymbol{\xi}(k) \approx 0$, the matrix $\boldsymbol{\Theta}(k)$ should be chosen such that $\Delta \boldsymbol{\phi}_j(k) - \boldsymbol{\Theta}(k) \Delta \mathbf{W}_j(k) \mathbf{z}_j(k) \approx 0$, or

$$\Delta \boldsymbol{\phi}_j(k) = \boldsymbol{\phi}_j(\mathbf{W}_j \mathbf{z}_j(k)) - \boldsymbol{\phi}_j(\hat{\mathbf{W}}_j(k) \mathbf{z}_j(k)) \approx \boldsymbol{\Theta}(k) \Delta \mathbf{W}_j(k) \mathbf{z}_j(k) \quad (65)$$

Noting that the activation functions in the vector $\boldsymbol{\phi}_j$ act element-wisely, therefore it is clearer to look at each element of the vector $\Delta \boldsymbol{\phi}_j(k)$. Its i^{th} element is denoted as $\Delta \phi_{j,i}(k) = \phi_{j,i}(\mathbf{w}_{j,ri} \mathbf{z}_j(k)) - \phi_{j,i}(\hat{\mathbf{w}}_{j,ri}(k) \mathbf{z}_j(k))$ where $\mathbf{w}_{j,ri}$, $\hat{\mathbf{w}}_{j,ri}(k)$ are the i^{th} rows of matrices \mathbf{W}_j , $\hat{\mathbf{W}}_j(k)$, respectively. Now let us look at the choice of $\boldsymbol{\Theta}(k)$ with different activation functions $\boldsymbol{\phi}_j$.

It is interesting to note that if the activation functions in the vector $\boldsymbol{\phi}_j$ are chosen as the ReLUs, which are defined as $\phi(x) = x$ if $x > 0$, and $\phi(x) = 0$ if otherwise. Hence, we have $\Delta \phi_{j,i}(k) =$

- $\Delta \mathbf{w}_{j,ri}(k) \mathbf{z}_j(k)$ if $\mathbf{w}_{j,ri} \mathbf{z}_j(k) \geq 0$ and $\hat{\mathbf{w}}_{j,ri}(k) \mathbf{z}_j(k) \geq 0$;
- 0 if $\mathbf{w}_{j,ri} \mathbf{z}_j(k) \leq 0$ and $\hat{\mathbf{w}}_{j,ri}(k) \mathbf{z}_j(k) \leq 0$;
- $\mathbf{w}_{j,ri} \mathbf{z}_j(k)$ if $\mathbf{w}_{j,ri} \mathbf{z}_j(k) \geq 0$ and $\hat{\mathbf{w}}_{j,ri}(k) \mathbf{z}_j(k) \leq 0$;
- $-\hat{\mathbf{w}}_{j,ri}(k) \mathbf{z}_j(k)$ if $\mathbf{w}_{j,ri} \mathbf{z}_j(k) \leq 0$ and $\hat{\mathbf{w}}_{j,ri}(k) \mathbf{z}_j(k) \geq 0$.

We consider the case in which $\mathbf{w}_{j,ri} \mathbf{z}_j(k)$ and

$\hat{\mathbf{w}}_{j,ri}(k) \mathbf{z}_j(k)$ are close to each other after the pre-training phase. Hence, in the last two cases above where they are of opposite signs, they should be sufficiently small. Therefore, it can be considered

that for these last two cases $\Delta\phi_{j,i}(k) \approx 0$. Hence, the matrix $\Theta(k)$ in (65) can be chosen as a diagonal matrix $\text{diag}\{\theta_1(k), \theta_2(k), \dots, \theta_{h_j}(k)\}$ where the diagonal elements are

$$\theta_i(k) = \begin{cases} 1 & \text{if } \hat{\mathbf{w}}_{j,ri}(k)\mathbf{z}_j(k) \geq 0 \\ 0 & \text{otherwise} \end{cases} \quad (66)$$

Looking back at (66), the value of $\theta_i(k)$ is actually the derivative of the ReLU function

$$\theta_i(k) = \hat{\phi}'_{j,i}(k) = \left. \frac{d\phi_{j,i}(x(k))}{dx(k)} \right|_{x(k)=\hat{\mathbf{w}}_{j,ri}(k)\mathbf{z}_j(k)} \quad (67)$$

Generalizing to any differentiable function, we set $\Theta(k) = \Phi'_j(k)$ with $\Phi'_j(k) = \text{diag}\{\theta_1(k), \theta_2(k), \dots, \theta_{h_j}(k)\}$ where $\theta_i(k)$ is defined in (67). With this first order approximation, we have

$$\phi_j(\mathbf{W}_j\mathbf{z}_j(k)) - \phi_j(\hat{\mathbf{W}}_j(k)\mathbf{z}_j(k)) \approx \Phi'_j(k)\Delta\mathbf{W}_j(k)\mathbf{z}_j(k)$$

Hence, equation (65) is satisfied. Now, replace the matrix $\mathbf{P}(k)$ into (51) and rewrite the full update law in (50) and (51) as follows

$$\hat{\mathbf{W}}_j^>(k+1) = \hat{\mathbf{W}}_j^>(k) + \alpha_1 \mathbf{L}(k)\mathbf{e}(k)\hat{\phi}_j^T(k) \quad (68)$$

$$\hat{\mathbf{W}}_j(k+1) = \hat{\mathbf{W}}_j(k) + \alpha_0 \Phi_j^{TT}(k)\hat{\mathbf{W}}_j^>T(k)\mathbf{L}(k)\mathbf{e}(k)\mathbf{z}_j^T(k) \quad (69)$$

It can be seen that these update laws are similar to the first order gradient descent when the activation functions at the output layer are linear.

The complete condition (62) can now be written as

$$\frac{2}{f_\sigma} \mathbf{L}(k) - \left(\alpha_1 \sum_{i=1}^{h_j} \hat{\phi}_{j,i}^2(k)\mathbf{L}^T(k)\mathbf{L}(k) + \alpha_0 \sum_{i=1}^{h_{j-1}} z_{j,i}^2(k)\mathbf{L}^T(k)\hat{\mathbf{W}}_j^>(k)\Phi'_j(k)\Phi_j^{TT}(k)\hat{\mathbf{W}}_j^>T(k)\mathbf{L}(k) \right) > 0 \quad (70)$$

4.3 Summary of Forward Progressive Learning Algorithm

The overall algorithm for learning of each SLFN in the FPL is described as follows:

- (i) The first phase: Pre-train the SLFN following the steps in subsection 4.1.
- (ii) The second phase: Fine-tuning of the SLFN:
 - (a) For each data sample $(\mathbf{z}_j(k), \mathbf{y}(k))$ in the training set:
 - (1) Calculate $\hat{\mathbf{y}}(k)$ using (45).
 - (2) Calculate $\mathbf{e}(k) = \mathbf{y}(k) - \hat{\mathbf{y}}(k)$.
 - (3) Update the weight matrices using update laws (68) and (69) where $\mathbf{L}(k)$ should satisfy (70).
 - (b) Move to the next training sample and repeat (a) (steps (1) to (3)) until all the samples in the training set have been used.
 - (c) When all the data samples in the training set have been used \rightarrow finish 1 loop. The training can take more than 1 loop if necessary.

5 Online Kinematic Control of Robot Manipulators

In this section, we show how the results can be adapted for online learning of robot kinematics without any modeling.

The rate of change of joint variables $\dot{\mathbf{q}}$ is related to the rate of change of position and orientation of the end effector in sensory space $\dot{\mathbf{x}}$ as

$$\dot{\mathbf{x}} = \mathbf{J}(\mathbf{q})\dot{\mathbf{q}} \quad (71)$$

where $\mathbf{J}(\mathbf{q})$ is the overall Jacobian matrix from joint space to sensory task space. The relationship in equation (71) can be approximated by a multilayer network whose output is given in equation (3)

$$\dot{\mathbf{x}} = \mathbf{J}(\mathbf{q})\dot{\mathbf{q}} = \mathbf{y}_{\mathcal{NN}}(\mathbf{W}_j|_{j=1}^n, \mathbf{q}, \dot{\mathbf{q}}) \quad (72)$$

It can be seen that the learning algorithms in section 3 and section 4 can be directly applied for offline learning by setting $\mathbf{y} = \dot{\mathbf{x}}$ and inputting to the network $\mathbf{q}, \dot{\mathbf{q}}$. However, for online robot control, a desired trajectory is specified and hence the learning algorithms need to be adapted for online learning purpose.

At the k^{th} step of online learning, we have

$$\dot{\mathbf{x}}(k) = \mathbf{J}(\mathbf{q}(k))\dot{\mathbf{q}}(k) = \mathbf{y}_{\mathcal{NN}}(\mathbf{W}_j|_{j=1}^n, \mathbf{q}(k), \dot{\mathbf{q}}(k)) \quad (73)$$

The estimated output of the network at the k^{th} step of online learning is given as

$$\hat{\dot{\mathbf{x}}}(k) = \hat{\mathbf{J}}(\mathbf{q}(k), \hat{\mathbf{W}}_{\Sigma}(k))\dot{\mathbf{q}}(k) = \mathbf{y}_{\mathcal{NN}}(\hat{\mathbf{W}}_j(k)|_{j=1}^n, \mathbf{q}(k), \dot{\mathbf{q}}(k)) \quad (74)$$

where $\hat{\mathbf{W}}_{\Sigma}(k)$ stands for all the estimated weight matrices $\hat{\mathbf{W}}_j(k)$ for $j = 1, 2, \dots, n$.

Let the reference joint velocity $\dot{\mathbf{q}}$ based on the sensory task space feedback be proposed as follows

$$\dot{\mathbf{q}}(k) = \hat{\mathbf{J}}^{\dagger}(\mathbf{q}(k), \hat{\mathbf{W}}_{\Sigma}(k))(\dot{\mathbf{x}}_d(k) - \alpha\Delta\mathbf{x}(k)) \quad (75)$$

where $\hat{\mathbf{J}}^{\dagger}(\mathbf{q}(k), \hat{\mathbf{W}}_{\Sigma}(k))$ is the pseudoinverse matrix of the estimated Jacobian $\hat{\mathbf{J}}(\mathbf{q}(k), \hat{\mathbf{W}}_{\Sigma}(k))$; α is a positive scalar; $\Delta\mathbf{x}(k) = \mathbf{x}(k) - \mathbf{x}_d(k)$; $\mathbf{x}_d(k)$ and $\dot{\mathbf{x}}_d(k)$, respectively, are the desired position and velocity of the end effector in the sensory task space. Premultiplying (75) by $\hat{\mathbf{J}}(\mathbf{q}(k), \hat{\mathbf{W}}_{\Sigma}(k))$ gives

$$\hat{\mathbf{J}}(\mathbf{q}(k), \hat{\mathbf{W}}_{\Sigma}(k))\dot{\mathbf{q}}(k) = \dot{\mathbf{x}}_d(k) - \alpha\Delta\mathbf{x}(k) \quad (76)$$

Subtracting (73) and (76) gives

$$\begin{aligned} & \mathbf{J}(\mathbf{q}(k))\dot{\mathbf{q}}(k) - \hat{\mathbf{J}}(\mathbf{q}(k), \hat{\mathbf{W}}_{\Sigma}(k))\dot{\mathbf{q}}(k) \\ = & \dot{\mathbf{x}}(k) - \dot{\mathbf{x}}_d(k) + \alpha\Delta\mathbf{x}(k) = \Delta\dot{\mathbf{x}}(k) + \alpha\Delta\mathbf{x}(k) \end{aligned} \quad (77)$$

Let $\boldsymbol{\varepsilon}(k) \triangleq \Delta\dot{\mathbf{x}}(k) + \alpha\Delta\mathbf{x}(k)$ be the online feedback error in online learning, from (73) and (74) we have

$$\boldsymbol{\varepsilon}(k) = \mathbf{y}_{\mathcal{NN}}(\mathbf{W}_j|_{j=1}^n, \mathbf{q}(k), \dot{\mathbf{q}}(k)) - \mathbf{y}_{\mathcal{NN}}(\hat{\mathbf{W}}_j(k)|_{j=1}^n, \mathbf{q}(k), \dot{\mathbf{q}}(k)) \quad (78)$$

Hence, the online feedback error $\varepsilon(k)$ here is equal to the output estimation error as seen in (46). By using $\varepsilon(k)$ for the update laws in section 4 to train the network, the convergence of this error can be guaranteed.

Remark: To simplify the analysis and presentation so as to gain better understanding, this paper considers the deep networks with sufficiently large number of neurons so that the reconstruction error is negligible. With the advances in hardware and computational technology in recent years, a large number of neurons and large number of layers can now be implemented by using computers with GPUs. However, it is important to note that in the presence of any approximation errors, the convergence to a bound can still be analyzed by extending the time domain results in [39] and the size of the bound is dependent on the approximation errors.

6 Case Studies

In this section, we present three case studies to illustrate the performance of the proposed learning algorithms. The first two are classification problems with the classical MNIST and CIFAR-10 databases. The third one is a regression problem with an online tracking control task for a UR5e manipulator.

6.1 MNIST Database

We considered the same network structure as in subsection 3.4, which was 784-300-100-50-10. We call it the full network. The activation functions used at hidden layers of this full network were ReLU $f(x) = \max(0, x)$ and at output layer were sigmoid $f(x) = 1/(1 + e^{-x})$.

With the structure of 784-300-100-50-10, the full network was trained through training three smaller single layer feedforward networks (SLFNs) sequentially: 784-300-10 (net I), 300-100-10 (net II), and 100-50-10 (net III). The activation functions used at the hidden layer of all three nets were the same as those at the hidden layers of the full network (ReLU), and the output activation functions of the three nets were also the same as those of the full network (sigmoid). Each SLFN was trained in 2 phases: pre-training using one-layer update and fine-tuning using two-layer update. In the pre-training phase of each net, the identity output was used, and in the fine-tuning phase, the sigmoid output was used. After net I (784-300-10) had been fully trained, its input weights (the layer 783-300) were kept and frozen, while its output weights (300-10) were discarded. This process creates a modified input layer which has a dimension of 300. This new input was fed into net II (300-100-10) and the training process of net II began. Similarly, after net II had been trained, a modified input layer of dimension 100 was created. Training of net III (100-50-10) took place afterwards.

The choice of gain matrices in pre-training phase of the three nets could be done similarly to the subsection 3.4, which is by calculating from the condition in (29). In fine-tuning phase, the gain matrix should satisfy the condition stated in (70). This condition seems to suggest that the training at the ending or fine-tuning stage should be done with a small gain so as to ensure convergence. In practice, the gain was initially set to some value, and then adjusted automatically by monitoring the condition in each update and reducing it if necessary.

The proposed FPL algorithm was compared with the SGD method where the network was trained for all layers together. We first tested the convergence of the FPL and SGD algorithms on an SLFN whose structure was the same as net I above by using various different gains (matrix \mathbf{L} in

Table 2: Convergence of FPL and SGD on net I with different gains

Gains	FPL	SGD
1000, 100, 10	converge	diverge
0.1, 0.01, 0.001	converge	converge

Table 3: Training & testing accuracy (%) by FPL and SGD for MNIST dataset

	FPL		SGD	
	training	testing	training	testing
Running 5 times	99.94	98.59	99.81	98.47
	99.93	98.37	99.81	98.30
	99.91	98.43	99.78	98.38
	99.92	98.38	99.81	98.26
	99.89	98.42	99.78	98.41
Mean values	99.92	98.44	99.80	98.36

FPL and learning rate in SGD). Since at this stage FPL iterates for 1 training example at a time, the batch size in the case of SGD was also set as 1 for consistency. Table 2 shows a summary of the results. Noting that for FPL, the gain matrix was for initial setting only since it can be adjusted automatically by checking the condition (70) during the training process. It is seen from the table that FPL can guarantee the convergence for a wide range of learning gain, while divergence can occur in SGD in cases where the gain is large. Another case study on online kinematic control of robot is presented in subsection 6.3.1 to illustrate the performance of FPL as compared to SGD in dealing with new tracking tasks or new circumstances.

After testing the convergence, we compared the training and testing accuracies of the two methods. The learning rate (LR) for SGD was chosen small enough such that the loss function converged. The LR was initially set at 0.05, the number of epochs was 100, and the batch size was 1. The LR was reduced by 2 after half of number of epochs and by 4 after 3/4 of number of epochs. For the FPL, the number of loops for training of the last layer in pre-training phase was 2. In the fine-tuning phases, the initial setting of the gain matrix for all nets was $\mathbf{L} = \text{diag}(0.01, \dots, 0.01)$. For each of the three nets, it took 28 loops with the gain scheduled to be decreasing when the loop number increased. To evaluate the effectiveness and consistency of the proposed method with different initial weights and random feed of training examples, we ran 5 times for each of FPL and SGD methods. The results in the 5 runs did not deviate much for both SGD and FPL. In each time, the accuracy for the test set was the maximum value (of the whole process with SGD, and of the process of training net III with FPL), and the accuracy for the training set was chosen at the epoch where the testing accuracy peaked. We then took average of the five values to get the mean training and testing accuracies.

The accuracies on training set and test set of the two methods are given in Table 3. It can be seen that the final test results of the FPL algorithm are quite similar to the corresponding results obtained by the SGD method.

Table 4: Testing accuracy (%) in FPL and SGD for CIFAR-10 dataset

	FPL		SGD	
	training	testing	training	testing
Running 5 times	94.49	88.24	94.41	88.20
	94.14	88.22	94.85	88.17
	93.98	88.12	94.17	88.14
	94.17	88.19	94.62	88.12
	94.41	88.19	94.78	88.20
Mean values	94.24	88.19	94.57	88.17

6.2 CIFAR-10 Database

For CIFAR-10 dataset, we used a pre-trained convolutional neural network (ResNet-18) to get the output of the convolutional part. This is one of the common techniques in transfer learning where the convolutional layers are fixed as feature extractor, and only the classifier layers are trained for the specific task. The output or extracted features were then considered as the input of the classifier part which was a network with several layers. The output of the convolutional part had a dimension of 512. The structure of the fully connected network was as follows.

- A 2-hidden layer network with structure 512-200-80-10 (200 units, 80 units in hidden layers). The activation functions at hidden layers are ReLU $f(x) = \max(0, x)$ and at output layer were sigmoid $f(x) = 1/(1 + e^{-x})$.

With the structure of 512-200-80-10, the full network was trained through training two smaller SLFNs sequentially: 512-200-10 (net I), 200-80-10 (net II).

The training and testing accuracies of the proposed method are compared with the SGD method. The SGD trains all layers of each network all together, with batch size set to be 1. The SGD method took 300 full epochs and LR = 0.01 initially. For the FPL algorithm, in the pre-training phase of the two nets, the number of loops for training of the last layer was 2. In the fine-tuning phases, the initial setting of the gain matrix for net I was $\mathbf{L} = \text{diag}(0.002, \dots, 0.002)$ and for net II was $\mathbf{L} = \text{diag}(0.0005, \dots, 0.0005)$. It took 128 loops for fine-tuning of net I and 68 loops for net II, and the gains were scheduled to be decreasing when the loop number increased. For each of FPL and SGD methods, we ran 5 times. In each time, the accuracy for the test set was the maximum value (of the whole process with SGD, and of the process of training net II with FPL), and the accuracy for the training set was chosen at the epoch where the testing accuracy peaked. We then took average of the five values to get the mean training and testing accuracies.

The accuracies on training set and test set of the two methods are given in Table 4. We can see that the final test results of FPL method are quite similar to the corresponding results obtained by SGD method.

6.3 Online Kinematic Control: UR5e Robot

Although it is good to ensure convergence of the deep learning systems in classifications problems so as to establish a systematic method instead of trial and error method for selection of learning gains, it may be sometimes arguable that the convergence analysis is not very critical in classification

problems since there is no harm to redo the training if divergence occurs. However, for online training of robots, convergence is crucial in assuring a safe operation at all time. In this section, we firstly show the importance of convergence in the online learning in robot control by comparing the performance of SGD and FPL on the simulator. After that, we show how a deep network can be built progressively by using FPL method such that the convergence of the online feedback error is guaranteed on the real robot. By repeating the operations, we shall show that the robot can gradually learn to execute a task based on feedback errors of the end effector without any knowledge of the kinematic model.

The tracking control task was drawing a circle in 3D space. The desired trajectory in sensory space is a circle (C1) specified as

$$\begin{aligned} x_1 &= -0.4 - 0.06 \cos(\omega t) - 0.18 \sin(\omega t) \\ x_2 &= 0.2 \cos(\omega t) - 0.02 \sin(\omega t) \\ x_3 &= 0.5 + 0.02 \cos(\omega t) + 0.06 \sin(\omega t) \end{aligned} \quad (79)$$

The units for the coordinates are meter (m). The circle (C1) has a center at $[-0.4, 0, 0.5]$ and a radius of 0.2 m.

6.3.1 Convergence tests of SGD and FPL on the simulator

Because of safety reason, we only tested SGD on the simulator as there is no guarantee of convergence when using SGD in online learning. For the purpose of comparison, FPL was also tested on the same simulator, before it was finally implemented on the actual robot (in subsection 6.3.2).

We considered the major axis which includes the first 3 joints q_1, q_2, q_3 . A single hidden layer network was built to approximate the Jacobian matrix of the UR5e robot through the relationship in (72). To do that, we firstly learned an SLFN with structure 3-12-3. That is, 3 input nodes (for q_1, q_2, q_3), 12 nodes in the hidden layer and 3 output nodes (for $\dot{x}_1, \dot{x}_2, \dot{x}_3$). The activation functions used for the hidden layers were modified softplus $f(x) = \log(0.8 + e^x)$ and for the output layer were identity $f(x) = x$.

Since the kinematic model is unknown, we needed to first manually move the robot around the desired trajectory in order to collect data for offline training of the network. The data of \mathbf{q} , $\dot{\mathbf{q}}$ and $\dot{\mathbf{x}}$ were collected during the manual movement. After getting the data, we trained the network offline by using SGD method. Different from the convergence test in the classification task, the learning rate here was chosen such that the offline learning converged. The obtained weights were then adopted as a starting point for the learning of Jacobian matrix in the online training.

We performed the online training using both SGD and FPL on the simulator of UR5e. The robot was first moved to an initial position so that the initial error was zero. The training was then conducted by using the online $\dot{\mathbf{q}}$ command as constructed in (75).

$$\dot{\mathbf{q}}(k) = \hat{\mathbf{J}}^\dagger(\mathbf{q}(k), \hat{\mathbf{W}}_\Sigma(k))(\dot{\mathbf{x}}_d(k) - \alpha \Delta \mathbf{x}(k))$$

The weights of the network were subsequently updated online using the SGD with estimation error $\dot{\mathbf{x}}(k) - \hat{\dot{\mathbf{x}}}(k)$ and the FPL with online feedback error $\boldsymbol{\varepsilon}(k)$ in (77). The matrix $\hat{\mathbf{J}}(\mathbf{q}(k), \hat{\mathbf{W}}_\Sigma(k))$ can be calculated based on current joint variables $\mathbf{q}(k)$ and current weights $\hat{\mathbf{W}}_\Sigma(k)$. With both methods, the same gain (learning rate) as used in the offline learning phase was used. To test the performance of the robot system in tracking new task, the desired speed of the end effector was increased (3-5 times) as compared to the original speed when moving the robot manually.

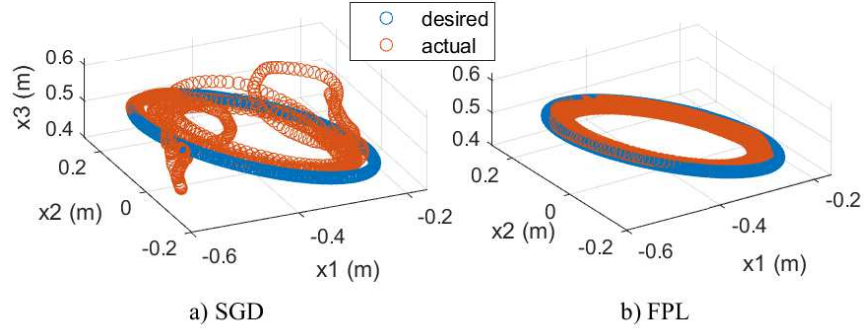


Figure 5: Desired and actual trajectories of the robot end-effector in the convergence test of online learning using SGD and FPL methods: a) SGD - Divergence occurred even though the same learning rate as in offline learning phase was used; b) FPL - Convergence was guaranteed by using the proposed online adjustment of gain matrix.

Fig. 5a shows the plot of the actual path of the robot end effector by using SGD to approximate the Jacobian matrix. It can be seen that the end effector deviates significantly from the desired path during the on-line training. The program was terminated after some time, as the learning of the network got unstable and caused the interruption in the calculation of $\hat{\mathbf{J}}^\dagger(\mathbf{q}(k), \hat{\mathbf{W}}_\Sigma(k))$.

The results in Fig. 5b shows that the convergence can be ensured by using FPL to achieve safe on-line training.

6.3.2 FPL on the real robot

With the real robot, the real values of joint variables \mathbf{q} and joint velocities $\dot{\mathbf{q}}$ were collected using the internal communication channel of the robot. The positions \mathbf{x} of the end effector in sensory space were recorded using a Kinect RGB-D camera. The sampling time was about 0.07 s. The velocities $\dot{\mathbf{x}}$ were then calculated from the positions \mathbf{x} .

For the experiment on real robot, the desired trajectory was also the circle (C1) specified at (79). The angular frequency (or angular speed) ω in (79) was planned in 5 phases. In the first 5 seconds, the desired ω is 0 rad/s, which aims to keep the robot at the initial position. The next 30 seconds (5 s - 35 s) is the acceleration period, when the desired angular frequency increases gradually from rest at 0 rad/s to full speed at $2\pi/30$ rad/s (2 rpm). After that, the robot end effector would move 3 rounds (revolutions) at full speed in 90 seconds (35 s - 125 s), before decelerating from full speed to 0 rad/s in the next 30 seconds (125 s - 155 s). Finally, the robot would be at rest for the last 5 seconds.

Training of the first hidden layer network We aimed to build a two-hidden layer network to approximate the Jacobian matrix of the UR5e robot through the relationship in (72). To do that, we firstly learned an SLFN with structure 3-12-3 (net I) (similar to the network used in the simulator above).

Though the proposed online kinematic control algorithm in section 5 can be applied directly, the transient performance at the initial stage of learning may not be good since the controller is completely model-free at the initial stage. To overcome this issue, we adopt a combination of offline and online trainings so that real-time feedback control using deep networks can be established

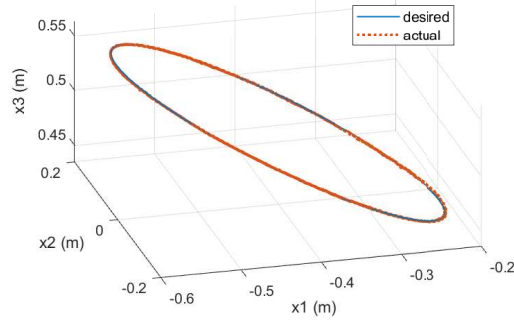


Figure 6: Desired and actual trajectories of the robot end-effector in sensory space for training cycle (C1).

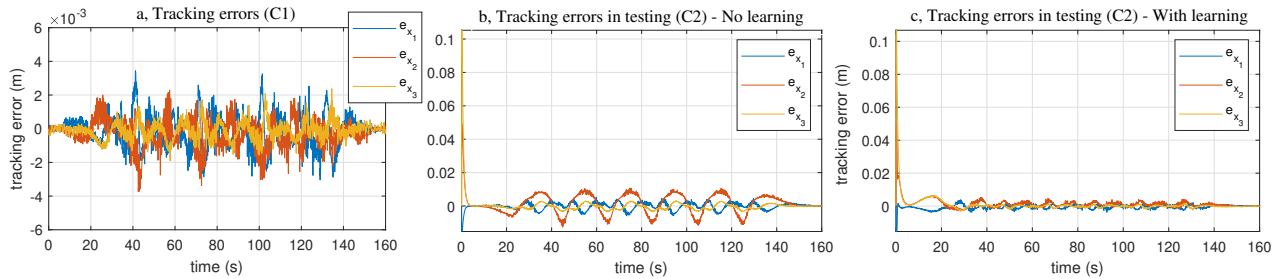


Figure 7: Performance of the online kinematic control task on the real UR5e robot. The first figure is for the training circle (C1): a, tracking error (with respect to time) of every coordinate. The last 2 figures are for the testing circle (C2): b, tracking errors when the weights of the network are fixed and c, tracking errors when the last layer of the network is updated.

eventually.

After getting the manual data, we first trained the network offline by one-layer pre-training (as in subsection 4.1) and two-layer fine-tuning (as in subsection 4.2). The obtained weights were then adopted as a starting point for the learning of Jacobian matrix in the online training.

For the online training, the robot was first moved to an initial position so that the initial error was zero. The training was then conducted by using the online $\dot{\mathbf{q}}$ command as constructed in (75). The weights of the network were subsequently updated online using the two-layer update with error $\varepsilon(k)$. The matrix $\hat{\mathbf{J}}(\mathbf{q}(k), \hat{\mathbf{W}}_{\Sigma}(k))$ can be calculated based on current joint variables $\mathbf{q}(k)$ and current weights $\hat{\mathbf{W}}_{\Sigma}(k)$.

Training of the second hidden layer network After the first net with one hidden layer had been trained, we discarded its output weights and then added one new hidden layer of 12 neurons. The structure of the whole network became 3-12-12-3. Because the input weights of this whole network were frozen, the training process was continued with a net of structure 12-12-3 (net II). The learning of this net was similar to that of net I. Again, offline training was first performed to avoid poor transient performance. The training data for offline training of net II were a combination of half of the amount of manual data and half of the amount of new data generated in the online

training of net I. After offline training, the online control task was done similarly to net I.

The desired and actual trajectories for online learning are shown in Fig. 6, and the tracking error is shown in Fig. 7a. It can be observed that the errors are very small and the actual trajectory follows the desired one very closely. This tells us that building network using FPL can guarantee the convergence of the tracking errors in online learning control.

Testing of the trained network To test the generalization property of the network, we used the Jacobian matrix obtained after online training of net II above for a tracking control task with a new trajectory which was also a circle (C2) with radius of 0.15 m. This circle was on a new plane which is 0.1 m lower along the x_3 -axis compared with (C1). The maximum speed of the movement was at $2\pi/20$ rad/s (or 3 rpm) and the direction of the movement was opposite.

Fig. 7b and 7c show the tracking errors for the new trajectory (C2). The initial errors for x_3 -axis are large (about 0.1 m) as the robot did not start on the new desired trajectory. The initial position of the end effector was set as the same as the old trajectory (C1) used for training. Fig. 7b shows the tracking errors when the Jacobian is used directly without any update of the weights. It can be seen that the peaks in the full-speed period (35 s - 125 s) are similar to each other (at about 0.01 m), which means that the errors are the same for each evolution of the movement of the end effector. This is understandable as the weights are kept constant during the new tracking control task. Fig. 7c shows the tracking errors when the Jacobian is updated during the online control. Only the weights of the last layer were trained during online learning. It is observed that the peaks in the full-speed period (35 s - 125 s) now are much smaller than the previous case.

Hence, from this case study, we can see that the FPL framework ensures the convergence of the tracking errors in the online learning. The framework also gives quite good generalization in this experiment and only the weights of the last layer are updated during online control task so as to achieve better tracking performance for the new trajectory.

7 Conclusion

In this paper, we have presented a layer-wise deep learning framework in which a multilayer feed-forward network can be built and trained such that the convergence of the algorithm is ensured. It has been shown that a robot can learn to execute an online kinematic control task in a safe and predictable manner without any modeling. The case studies of classification tasks using MNIST and CIFAR-10 databases have shown that using the learning framework can result in similar accuracies as compared to the gradient descent method while ensuring convergence. The proposed method would widen the potential applications of deep learning in the areas of robotics and control.

References

- [1] W. T. Miller, "Real-time application of neural networks for sensor-based control of robots with vision," *IEEE Trans. Syst., Man, Cybern.*, vol. 19, no. 4, pp. 825–831, 1989.
- [2] K. Hornik, M. Stinchcombe, and H. White, "Multilayer feedforward networks are universal approximators," *Neural Netw.*, vol. 2, no. 5, pp. 359–366, 1989.
- [3] T. Poggio, A. Banburski, and Q. Liao, "Theoretical issues in deep networks," *Proc. Natl. Acad. Sci.*, 2020.

- [4] K. S. Narendra and K. Parthasarathy, "Identification and control of dynamical systems using neural networks," *IEEE Trans. Neural Netw.*, vol. 1, no. 1, pp. 4–27, 1990.
- [5] R. Sanner and J.-J. Slotine, "Gaussian networks for direct adaptive control," *IEEE Trans. Neural Netw.*, vol. 3, no. 6, pp. 837–863, 1992.
- [6] C. Yang, Z. Li, R. Cui, and B. Xu, "Neural network-based motion control of an underactuated wheeled inverted pendulum model," *IEEE Trans. Neural Netw. Learn. Syst.*, vol. 25, no. 11, pp. 2004–2016, 2014.
- [7] X. Li and C. C. Cheah, "Adaptive neural network control of robot based on a unified objective bound," *IEEE Trans. Control Syst. Technol.*, vol. 22, no. 3, pp. 1032–1043, 2014.
- [8] W. He, Y. Chen, and Z. Yin, "Adaptive neural network control of an uncertain robot with full-state constraints," *IEEE Trans. Cybern.*, vol. 46, no. 3, pp. 620–629, 2016.
- [9] C. Yang, Y. Jiang, Z. Li, W. He, and C.-Y. Su, "Neural control of bimanual robots with guaranteed global stability and motion precision," *IEEE Trans. Ind. Informat.*, vol. 13, no. 3, pp. 1162–1171, 2016.
- [10] R. A. Licitra, Z. I. Bell, and W. E. Dixon, "Single-agent indirect herding of multiple targets with uncertain dynamics," *IEEE Trans. Robot.*, vol. 35, no. 4, pp. 847–860, 2019.
- [11] S. Lyu and C. C. Cheah, "Data-driven learning for robot control with unknown jacobian," *Automatica*, vol. 120, p. 109120, 2020.
- [12] F.-C. Chen and H. Khalil, "Adaptive control of a class of nonlinear discrete-time systems using neural networks," *IEEE Trans. Automat. Contr.*, vol. 40, no. 5, pp. 791–801, 1995.
- [13] F. L. Lewis, A. Yesildirek, and K. Liu, "Multilayer neural-net robot controller with guaranteed tracking performance," *IEEE Trans. Neural Netw.*, vol. 7, no. 2, pp. 388–399, 1996.
- [14] R. Fierro and F. L. Lewis, "Control of a nonholonomic mobile robot using neural networks," *IEEE Trans. Neural Netw.*, vol. 9, no. 4, pp. 589–600, 1998.
- [15] L. Cheng, Z.-G. Hou, and M. Tan, "Adaptive neural network tracking control for manipulators with uncertain kinematics, dynamics and actuator model," *Automatica*, vol. 45, no. 10, pp. 2312–2318, 2009.
- [16] C. M. Bishop *et al.*, *Neural networks for pattern recognition*. Oxford university press, 1995.
- [17] X. Glorot, A. Bordes, and Y. Bengio, "Deep sparse rectifier neural networks," in *Proc. 14th Int. Conf. Artif. Intell. Statist.*, 2011, pp. 315–323.
- [18] Y. Bengio *et al.*, "Learning deep architectures for AI," *Found. Trends Mach. Learn.*, vol. 2, no. 1, pp. 1–127, 2009.
- [19] H. Mhaskar, Q. Liao, and T. Poggio, "When and why are deep networks better than shallow ones?" in *Thirty-First AAAI Conf. Artif. Intell.*, 2017, p. 2343–2349.
- [20] H. N. Mhaskar and T. Poggio, "Deep vs. shallow networks: An approximation theory perspective," *Anal. Appl.*, vol. 14, no. 06, pp. 829–848, 2016.

- [21] I. Goodfellow, Y. Bengio, and A. Courville, *Deep learning*. MIT press, 2016.
- [22] J. Schmidhuber, “Deep learning in neural networks: An overview,” *Neural Netw.*, vol. 61, pp. 85–117, 2015.
- [23] D. E. Rumelhart, G. E. Hinton, and R. J. Williams, “Learning representations by back-propagating errors,” *Nature*, vol. 323, no. 6088, pp. 533–536, 1986.
- [24] Y. LeCun, Y. Bengio, and G. Hinton, “Deep learning,” *Nature*, vol. 521, no. 7553, p. 436, 2015.
- [25] A. Krizhevsky, I. Sutskever, and G. E. Hinton, “Imagenet classification with deep convolutional neural networks,” in *Adv. Neural Inform. Process. Syst.*, 2012, pp. 1097–1105.
- [26] T. J. Sejnowski, “The unreasonable effectiveness of deep learning in artificial intelligence,” *Proc. Natl. Acad. Sci.*, 2020.
- [27] P. Guo and M. R. Lyu, “A pseudoinverse learning algorithm for feedforward neural networks with stacked generalization applications to software reliability growth data,” *Neurocomputing*, vol. 56, pp. 101–121, 2004.
- [28] K.-A. Toh, “Analytic network learning,” *arXiv:1811.08227*, Nov, 2018.
- [29] H.-T. Nguyen, C. C. Cheah, and K.-A. Toh, “A data-driven iterative learning algorithm for robot kinematics approximation,” in *2019 IEEE/ASME Int. Conf. Adv. Intell. Mechatronics (AIM)*. IEEE, 2019, pp. 1031–1036.
- [30] Y. Bengio, P. Lamblin, D. Popovici, and H. Larochelle, “Greedy layer-wise training of deep networks,” in *Adv. Neural Inf. Process. Syst.*, 2007, pp. 153–160.
- [31] D. Erhan, Y. Bengio, A. Courville, P.-A. Manzagol, P. Vincent, and S. Bengio, “Why does unsupervised pre-training help deep learning?” *J. Mach. Learn. Res.*, vol. 11, no. Feb, pp. 625–660, 2010.
- [32] C. Hettlinger, T. Christensen, B. Ehlert, J. Humpherys, T. Jarvis, and S. Wade, “Forward thinking: Building and training neural networks one layer at a time,” *arXiv:1706.02480*, 2017.
- [33] N. Sünderhauf, O. Brock, W. Scheirer, R. Hadsell, D. Fox, J. Leitner, B. Upcroft, P. Abbeel, W. Burgard, M. Milford *et al.*, “The limits and potentials of deep learning for robotics,” *Int. J. Robot. Res.*, vol. 37, no. 4-5, pp. 405–420, 2018.
- [34] G. Montavon, W. Samek, and K.-R. Müller, “Methods for interpreting and understanding deep neural networks,” *Digit. Signal Process.*, vol. 73, pp. 1–15, 2018.
- [35] D. Gunning, M. Stefik, J. Choi, T. Miller, S. Stumpf, and G.-Z. Yang, “XAI—explainable artificial intelligence,” *Science Robotics*, vol. 4, no. 37, 2019.
- [36] D. Gunning, “Explainable artificial intelligence (XAI),” *Defense Advanced Research Projects Agency (DARPA), nd Web*, vol. 2, 2017.
- [37] Y. LeCun, L. Bottou, Y. Bengio, and P. Haffner, “Gradient-based learning applied to document recognition,” *Proc. IEEE*, vol. 86, no. 11, pp. 2278–2324, 1998.

- [38] A. Krizhevsky *et al.*, “Learning multiple layers of features from tiny images,” 2009.
- [39] S. Kawamura, F. Miyazaki, and S. Arimoto, “Is a local linear pd feedback control law effective for trajectory tracking of robot motion?” in *Proc. 1988 IEEE Int. Conf. Robot. Automat.* IEEE, 1988, pp. 1335–1340.